A CELLULAR DEVICE

TO TARGET CANCER CELLS

A THESIS SUBMITTED TO

THE GRADUATE SCHOOL OF ENGINEERING AND SCIENCE OF

BILKENT UNIVERSITY

IN PARTIAL FULFILLMENT OF THE REQURIMENTS FOR THE

DEGREE OF

MASTER OF SCIENCE

IN

MATERIALS SCIENCE AND NANOTECHNOLOGY

BY

JULIAN OSTAKU

OCTOBER 2021

A CELLULAR DEVICE TO TARGET CANCER CELLS

By Julian Ostaku

October 2021

We certify that we have read this dissertation and that in our opinion it is fully adequate, in scope and in quality, as a thesis for the degree of Master of Science.

Urartu Özgür Şafak Şeker (Advisor)

Serkan İsmail Göktuna

Ceren Özkul Koçak

Approved for the Graduate School of Engineering and Science:

Ezhan Karaşan

Director of the Graduate School

ABSTRACT

A CELLULAR DEVICE TO TARGET CANCER CELLS

Julian Ostaku

M.Sc. Materials Science and Nanotechnology

Advisor: Urartu Özgür Şafak Şeker

October 2021

Cancer is the second leading cause of death globally, affecting one out of three people during their lifetime. Due to its severity and high incidence, numerous treatment methods have been implemented, with the Chimeric Antigen Receptor T-Cell (CAR-T) therapy remaining the most promising one. Other therapy options such as surgery, chemotherapy and radiation therapy remain the backbone of cancer treatment, however these therapies are not effective enough as they do not discriminate among the healthy and cancerous tissues. Therefore, there is an imperative need in developing novel cancer treatment therapies that offer precise localization and on target therapeutics release.

In this study, we aim to develop an engineered bacterial device, that can sense Jimt1 breast cancer cells, which are characterized by overexpression of human epidermal growth factor receptor 2 (HER2). 2Rs15d, a nanobody that binds to HER2 receptor, is expressed on the surface of *Escherichia coli* BL21 (DE3) via Ag43 autotransporter protein. Upon localization in the tumor site, a therapeutic agent will be released on the

outer surface. By creating this platform, we aim to target the main problems of the existing cancer therapies.

Keywords: Living therapeutics, breast cancer cells, HER2, secretion, nanobody.

ÖZET

TÜMÖRLERİ HEDEFLEMEK İÇİN HÜCRESEL BİR CİHAZ

Julian Ostaku

Malzeme Bilimi ve Nanoteknoloji, Yüksek Lisans

Tez Danışmanı: Urartu Özgür Şafak Şeker

Ekim, 2021

Dünya çapındaki ölümlerin sebepleri arasında ikinci sırada yer alan kanser hastalığı, üç insandan birini etkilemektedir. Hastalığın ciddiyeti ve yaygınlığı sebebiyle, en umut vadedenlerden biri Kimerik Antijen Reseptörü T hücreleri (Chimeric Antigen Receptor T-Cell/ CAR-T) olmak üzere çeşitli tedavi yöntemleri yürütülmüştür. Cerrahi, kemoterapi ve radyoterapi gibi diğer seçenekler tedavinin temelini oluştursa da sağlıklı doku ile kanser dokusunu etkili şekilde ayıramamaları yönüyle yeterli derecede verimli olamamaktadır. Bu yüzden kanseri lokalize eden ve ilgili bölgeye hedef terapötiklerin salınımını sağlayan yenilikçi kanser terapilerinin geliştirilmesi büyük önem taşımaktadır.

Bu çalışmada, HER2 reseptörünün aşırı ifade edildiği Jimt1 meme kanseri hücre hattını algılayan bir programlanmış bakteri geliştirmeyi hedefledik. Bu amaçla, HER2 reseptörüne bağlanan 2Rs15d nano parçacıkları *E. Coli* BL21 (DE3) yüzeyinde ifade

edildi. Nanoparçacıkların *E. coli* yüzeyinde ifadesi için oto-taşıyıcı Ag43 proteini kullanıldı. Bakteri hücrelerinin tümör bölgesinde lokalizasyonu sağlandıktan sonra, hücre dışına salacakları terapatik protein ile tümör inhibisyonu hedeflenmektedir.

Anahtar Kelimeler: Canlı terapötikler, meme kanseri hücreleri, HER2, salgı, nanobody.

ACKNOWLEDGEMENT

First of all, I would like to express my sincere gratitude to my supervisor Dr. Urartu Özgür Şafak Şeker who has guided and encouraged me during all this experience. I am grateful to him for giving me the chance to work at his laboratory and teaching me a lot during all these years. I would also like to thank my jury members, Dr. Ceren Özkul Koçak and Dr. Serkan İsmail Göktuna for their valuable and helpful comments during the revision process of my thesis.

I want to thank my project collaborators, Recep Erdem Ahan and Dr. Ebru Şahin Kehribar for their significant help throughout this study. I would especially like to thank Recep for sharing his knowledge and helping me adapt to this work since the moment I joined the lab. Moreover, I would like to thank all the current and past members of this laboratory who have made my stay here entertaining. I want to thank Ahmet Hınçer, Anooshay Khan, Dr. Behide Saltepe, Busra Merve Kırpat, Dr. Ebru Aras, Dr. Elif Duman, Celif Cemile Elif Özçelik, Çisil Köksaldı, Eray Ulas Bozkurt, Merve Erden Tucer, Murat A. Güngen, Nedim Hacıosmanoğlu, Gökçe Özkul, Gizem Makas, Nedim Kurt, Suat Tüçer and Gozeel Binte Shahid who helped me a lot this last semester.

I want to thank Merve for the joyful time we spent during our experiments breaks, all her support and her consistency in calling me early in the morning to wake me up. Sila was the person with whom I spent most of my best times in here. I want to thank her for all the fun, and quality time as well as all the support in my studies. Ozge Begli was the first to leave the lab due to her graduation but was one of the best people I have met

here. I want to thank her for her great friendship, as well as her meaningful advice whenever things got rough.

Lastly, I want to thank my family for everything they have done for me. I want to thank my father Flamur, my mother Dylbere, my brothers Perparim and Armend as well as my grandfather Dylaver. They have been my main support system for everything I have done until know and I’m very grateful to them for that. Moreover, I would like to thank Naxhije for all the quality time we have spent together and Tian for simply being the best.

This project was partially funded by TUBITAK project 115M108.

TABLE OF CONTENTS

LIST OF FIGURES

LIST OF TABLES

CHAPTER 1

1. INTRODUCTION

1.1 Living therapeutics and synthetic biology

Synthetic biology offers the means for the construction of novel biological parts that can have various purposes (1). Even though being frequently considered as an emerging field, in the intersection of biology and engineering, it has eventually been consolidated by extensively expanding the toolbox of genetic parts that can be implemented in a vast number of organisms. Using the tools offered by synthetic biology living therapeutics have been designed to detect different targets, produce therapeutics, and deliver them on site. Originally, living therapeutics dates back to 1867 when Busch, a medical physician observed that his patient, who was suffering from cancer, went into remission after contracting a *Streptococcus pyogenes* infection (2). Twenty-four years later, William Coley, a medical physician, injected *Streptococcus* bacteria directly to the tumor site of one of his patients in order to ignite an immune response which would affect and eventually kill the cancer cells. Based on his strategy he was able to help his patient and extend his lifespan for eight more years (3). Unfortunately, many of his patients also passed away due to complications arising from the infection, and in order to solve the problem he started injecting a mixture of dead bacteria to his patients which later on came to be known as Coleys Toxins (4).

The new generation of living therapeutics is mostly based on engineering microbial organisms that consists of integrated sensing mechanisms which can respond to different

biomarkers (5), temperature (6), chemicals (7), hypoxia (8), pH (9), microenvironmental topologies etc. as well as genetic toolboxes that can mediate on situ therapeutics release.

1.2 Living therapeutics and cancer

According to World Health Organization (WHO) cancer causes 9,6 million deaths every year and considering the statistics it is the second deadliest disease on Earth (10). The main modes of cancer treatment nowadays remain surgery, chemotherapy and radiotherapy which besides being considerably effective have their own drawbacks (11). These modes of cancer treatment lack specificity due to the fact that they indiscreetly attack healthy tissues as well, causing irreversible damage. Therefore, there is an imperative need to address alternative solutions that would incorporate specific localization and controlled therapeutic release into the tumor site. To achieve specific localization and in situ drug release synthetic biology has been used to modify microbial organisms so that they can localize on the tumor site and release the therapeutics in a controlled manner. The most used organism for treatment of cancer via living therapeutics remains *E. coli* Nissle 1917, which is a non-pathogenic strain of *E. coli* that does not cause septic shock. Besides Nissle, *Lactococcus lactis* (12) and attenuated versions of *Salmonella typhimurium* (13) have also been tested as living therapeutics agents to target cancer. Three main steps remain crucial when engineering living therapeutics: (I) Selection of the organism, (II) Localization of the tumor site, (III) Mode of therapeutics delivery.

1.3 Organisms used as living therapeutics to target tumors

When it comes to selecting a bacterium to attack tumor site, two different strategies can be followed. The first one would be choosing bacteria that would preferentially localize and grow into the tumor site and on its own would cause oncolysis, whereas the second strategy would be to engineer bacteria so that they can localize themselves in the tumor site and produce on site anti-tumor therapeutics.

One of the most well-known organisms chosen for the first strategy is *Salmonella*. These are facultatively anaerobe bacteria that selectively grow into the tumor site. It has been shown that systematic administration of *Salmonella* induces immune cell activation and therefore their infiltration into the tumor site which results in attacking the tumor cells (14). How exactly it induces the immune system remains unclear, but it is hypothesized that it down-regulates AKT/mTOR pathway resulting in autophagy and/or activates Caspase 3 which results in apoptosis (15).

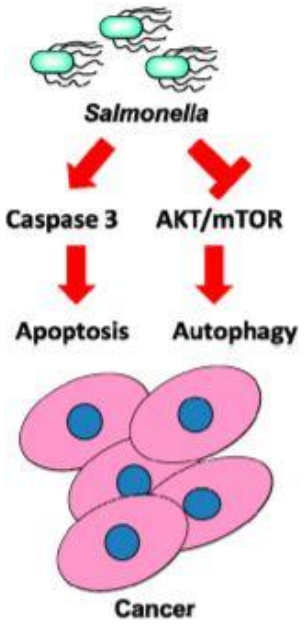

Figure 1. Salmonella down-regulates AKT/mTOR pathway resulting in autophagy and/or activates Caspase 3 which results in apoptosis (15).

Even though this seems like a proper solution, *Salmonella* is a pathogen which causes a high number of deaths every year, therefore genetic engineering is required for safe administration of this strain as living therapeutics cargo to treat tumors (16). Regarding the second strategy species such as *E. coli* are generally preferred due to their genetic plasticity. Other than that, species from *Clostridium, Lactobacillus, Listeria, Bifidobacterium* genus have been engineered and eventually tested (17). Attenuated version of *Salmonella typhimurium* was genetically engineered to be auxotrophic for leucine and arginine. This strain showed to be effective towards a various number of cancers that were tested (18).

1.4 Targeting tumor microenvironment

For the detection of tumors via bacteria different strategies have been proposed and tested. In general, all these strategies tend to take advantage of various specific cues of the tumor microenvironment. Such cues involve pH, hypoxia, glucose, lactate etc.

To detect hypoxia different promoters sensitive to oxygen such as pepT and FF20 have been used (19,20). pepT is an oxygen sensitive promoter that is regulated by fumarate and FNR (nitrate reduction regulatory protein). Under hypoxic conditions FNR forms an active homodimer activating the promoter, whereas on the presence of oxygen it exists in an inactive monomer form (21). Using this property specific cargo proteins could be cloned under the control of this promoter so that they would potentially be expressed only at the hypoxic environments. Under normal conditions the pH of the blood would

be 7,4 (22) whereas in the tumor microenvironment in various cases pH can fluctuate between 5,5 to 7,0 (23). Using this property promoters regulated by pH have been tested for tumor targeting. pCadC, a promoter that is regulated by CadC protein which increases activity in acidic environments was used to control the expression of *asd* gene in an *asd*-knockout *E. coli* (24). *Asd* gene produces an enzyme important for lysine, methionine, and arginine synthesis in *E. coli* therefore its downregulation would cause bacterial death (25). Using this construct Danino et. al were able to show an increased localization of *E. coli* in tumor site on mice. Similarly, they designed a lactate sensitive pLldR promoter which took advantage of the lactate signatures of tumor microenvironment, and they had similar results (24). Promoters sensitive to glucose gradient in the tumor mass have also been engineered. In a study by Forbes et. al the researchers built a biosensor sensitive to glucose gradient and transformed it to *E. coli* K12. They tested their construct in a tumor mass microfluidic chip and concluded that their design can be used for identification of local tumor cell viability (26).

1.5 Targeting cancerous cells via living therapeutics

Despite the tumor microenvironment, cancerous cells also develop biomarkers levels of which may differentiate them from healthy cells. One of these biomarkers is programmed cell death ligand 1 (PD-L1), which is upregulated in cancerous cell. It binds to programmed cell death protein 1 (PD-1) which is expressed on T and B immune cells, rendering it undetectable to the immune system. The binding results in tolerance and dysfunction of T-cells (26,28). Therefore, blocking this biomarker has been tested widely by synthetic biology. *E. coli* Nissle has been designed to produce and release, via cell lysis, PD-L1 blocking nanobodies. In vivo studies have shown that this

method had better results compared to traditional antibodies administration (29). In another study an attenuated *Salmonella* strain was engineered to display an Arg-Gly-Asp peptide on its surface. This peptide has high specificity towards $a_v b_3$ integrin which is overexpressed on the surface of tumor cells (30,31). The study showed enhanced localization of the engineered bacteria on the MDMA-MB-231 and MDA-MB-435 tumor sites as well as considerable tumor regression. Moreover, *Salmonella typhimurium* VNP has been engineered to express carcinoembryonic antigen (CEA)-specific single chain antibody fragment on its surface which has resulted in enhanced localization of this bacteria in the tumor site of CEA-expressing transgenic mice (32).

1.6 Synthetic adhesins

Synthetic adhesins can be constructed and used to target different biomarkers that are overexpressed on the surface of different cancerous cells. The work of Piñeero-Lambea et al. (33) on this topic created a modular platform with different synthetic adhesins that can be expressed on surface of *E. coli* and be used to target various cancer cell types. The synthetic adhesins created in his study consist of a modular structure that has a stable β domain, which mediates the outer membrane localization, and a surface exposed immunoglobulin domain with high affinity, stability and solubility that can be chosen from various libraries (33).

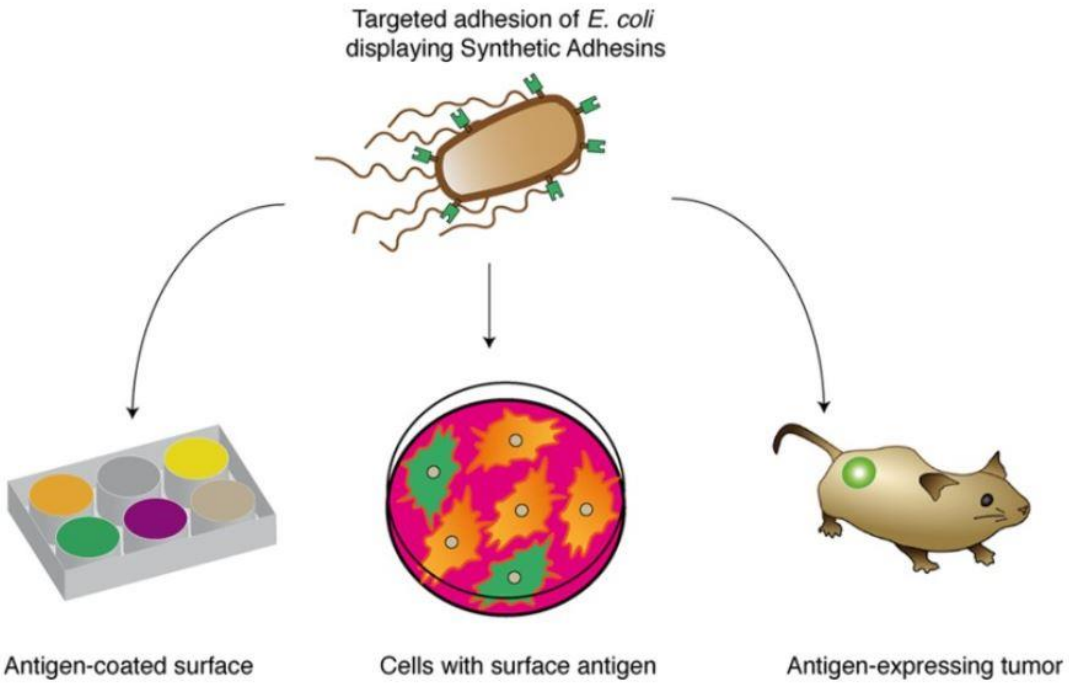

Figure 2. Schematic representation of the design and evaluation of synthetic adhesins Piñeero-Lambea et.al (33).

1.7 Payloads and strategies for bacteria mediated drug release

With the development of more sophisticated gene circuit designs, various drug delivery strategies have been implemented in tumor targeting bacterial devices. Once engineered bacteria reach the tumor microenvironment (TME), expression of precisely controlled payloads can maximize the delivery efficiency to tumor cells. Expression of the drug-encoding gene inside the bacterial cell can be activated with internal and external factors as well as feedback mechanisms. Specific conditions of TME can be utilized as external triggers by implementing hypoxia sensitive promoters upstream of drug-encoding gene (34) or utilizing inducible systems activated under acidic conditions (35).

Since targeted bacteria species will preferentially colonize at the tumor sites, quorum sensing can be used as self-triggering agent, adding a control layer between localization and delivery steps. Quorum sensing bacteria expresses a natural autoinducer, acyl homoserine lactone (AHL), which binds and activates the transcription factor LuxR in high density cultures. Activated LuxR then can activate the expression of specific genes under the control of its cognate promoter, and this provides a mechanism for bacteria to further adapt dynamic environmental conditions. This mechanism can be utilized for adjusting both time and the dosage parameters of the cancer targeting bacterial device. In fact, QS systems were implemented successfully in many bacteria-colonizing tumors (36,38). Once the strategies for highly targeted localization and tightly controlled delivery mechanism are established, the therapeutic agent can be selected for enhancing the bacteria-based cancer therapy. Up to now, various cytotoxic agents, prodrug-converting enzymes, immune regulators, tumor stroma-targeting molecules, and siRNAs have been put into test. Cytotoxic agents implemented in a strictly controlled system, can be secreted from bacterial cells to inhibit nearby tumor activities. For example, Cytolysin A (ClyA) is a 34 kDa pore-forming hemolytic protein and it was employed in different hosts including *E. coli* and attenuated *S. Typhimurium.* It showed excellent potential in tumor inhibiting properties combined with arabinose or doxycycline inducible systems (38,39).

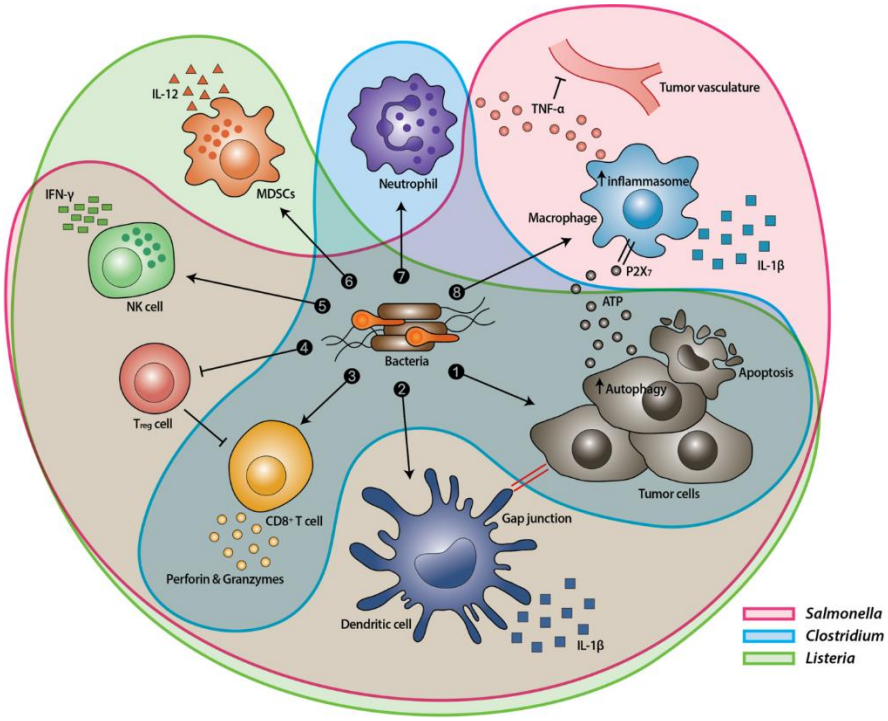

Figure 3. The effects of cancer-combatting bacterial cells on the TME (40). **1.** Bacteria can secrete toxins to induce apoptosis or autophagy. **2.** Interaction with bacterial components can lead DCs to secrete proinflammatory cytokine IL-1β which then activates CD8+ T cells. **3.** Bacterial flagellin can further enhance antitumor response of the activated CD8+ T cells. **4.** Flagellin and TLR5 signaling can also improve antitumor acitivity of CD8+ T cells by decreasing the number Treg cells. **5.** *S. Typhimurium* flagellin can also help NK cells to stimulate interferon-γ (IFN-γ). **6.** Listeria-infection of MDSCs can induce a phenotypical change which can further enhance $CD8^+$ T and NK cell responses **7.** *S. Typhimurium* and *Clostridium* infections can lead to neutrophil accumulation which increases the immune response. **8.** The elevated secretion of IL-1β and TNF-α can also be achieved through activated macrophage inflammasome. Bacterial components such as LPS and flagellin and damaged cancer cells can activate the macrophage inflammasome. NK cell: natural killer cell. T_{reg} cell: regulatory T cell.

MDSCs: myeloid-derived suppressor cells. $P2X_7$ receptor: purinoceptor 7-extracellular ATP receptor. LPS: lipopolysaccharide

1.8 Aim of the study

It is well-known that the current therapeutics employed for cancer treatment have introduced challenges such as systematic toxicity, drug resistance, and failing to completely cure the target tissue. Recent advances in bacteria-based therapeutic strategies offer promising new tools to overcome these limitations as well as maximizing the efficiency of the chemotherapeutic agents deployed in the conventional treatment options. In this study we aimed to develop a cellular device for targeting and killing Jimt1 breast cancer cells. A nanobody specific to HER2 receptor would be expressed at the surface of *E. coli* BL21 (DE3). By taking advantage of the nanobody we hypothesized that our bacteria would localize into the tumor site. Upon localization, the bacteria would release a therapeutic to kill Jimt1 breast cancer cells. By building this two-step approach we aimed to target the specificity and *in situ* drug release problems of the existing cancer therapies.

CHAPTER 2

2. MATERIALS AND METHODS

2.1 Bacterial strains growth, storage, maintenance, and transformation

In this project, *E. coli* DH5α PRO, which contains a cassette providing spectinomycin resistance, was used to perform cloning experiments, and *E. coli* BL21 (DE3) was used for protein expression. For cell stock preparation equal volumes of cell culture grown overnight at Lysogeny Broth (LB) medium and 50% (v/v) Glycerol were mixed and stored at -80°C. Bacterial cells were grown in Lysogeny Broth medium (LB) consisting respective antibiotic (1:1000) at 37°C overnight (o/n) at 200 rotations per minute (rpm). Throughout this study chemical transformation was performed. To prepare chemical competent cells bacteria were grown overnight and then diluted 1:100 in fresh LB with appropriate antibiotics and grown 37°C at 200 rpm till OD_{600} reached 0.4. After that, cells were cooled on ice for 10 minutes and then collected by centrifuging at 1000 g for 10 minutes at 4°C. Pellet was dissolved in TSS buffer (1:10 of the diluted culture volume). 100µl aliquots were transferred to 1.5 ml micro-centrifuging tubes and stored at -80°C for prospective usage. To chemically transform the cells, competent cells were thawed on ice for 30 minutes and then intact plasmid (100 ng) or Gibson Assembly mixture was added. Afterwards cells were incubated for another 20 minutes on ice and then heat shocked at 42°C for 45 seconds. After heat shock, cells were incubated on ice for 2 minutes and after adding 500 µl of fresh LB to the samples, they were incubated at 37°C, 200 rpm for 45 minutes. After incubation, the samples were centrifuged at 5500 g for 6 minutes and 400 µl of the supernatant was removed. The pellet was resuspended in

the remaining volume and spread on LB agar plates consisting of the adequate antibiotics. LB agar plates were grown o/n at 37°C incubator properly grown colonies were collected.

2.2 Constructs design and cloning

2.2.1 Cloning via Gibson Assembly

Parts for cloning were obtained as Polymerase Chain Reaction (PCR) products or Restriction Digestion Reaction products. To verify the parts size gel electrophoresis was performed in 1% agarose gel. Gels were run at 120V for 45 minutes and size was determined by visualization under blue light and comparing with the 2log DNA ladder. Afterwards gel extraction procedure was performed using MN PCR clean-up kit following the accompanying protocol of the kit. The isolated parts where then assembled using Gibson Assembly homemade reaction mixture. The reaction mixture consisted of 7,5 µL of 1,33X Gibson mix and it was completed to a total volume of 10 µL by adding 50 ng of the backbone dissolved in double distilled water (ddH_2O) and equal molar of insert. The sample was stored at +50°C for 60 minutes and at the end the solution was transformed to chemically competent *E. coli* DH5α PRO following the steps mentioned in the previous paragraph.

2.2.2 Plasmid design and sequence alignment using benchling

Benchling is a platform to work on DNA sequences, analyze sequence data and make new designs. Sequence data and information can be recorded by using new project- new DNA/ AA (amino acid) sequence tab on the left panel. Users can copy, cut and paste the sequence of interest. Annotations can be added by entering the positions of the parts

such as promoters, ribosome binding sites or open reading frame. It is possible to show the restriction sites and run a virtual digest indicating the expected bands on the gel by using a single restriction enzyme or a combination of enzymes. Additionally, sequence data (. ab1) can be annealed with the sequence of interest and custom parameters can be set using the sequence alignment tool on the right panel. Matching sequences appear in grey color on the linear map at the bottom op page while mismatches are indicated in red color. Gaps and ambiguous reads are marked on the reference sequence.

2.2.3 Polymerase chain reaction (PCR)

PCR method enables the amplification of certain regions on the DNA within the borders defined by two primers for several applications such as DNA sequencing and cloning. The reaction is based on the denaturation of DNA upon heating followed by formation of new strands by DNA polymerase upon binding of forward and reverse primers at lower temperatures. The reaction requires a heat resistant DNA polymerase, a buffer for enzyme activity, dNTPs as building blocks, a pair of primers and a DNA template. Conditions for the reaction are as followed:

1	2	3	4	5	6
Initial denaturation	Denaturation	Annealing	Elongation	Final Elongation	On hold
95°C	95°C	Annealing temperature *	72°C	72°C	4°C
30 seconds	10 seconds	30 seconds	30 seconds/kb	2 minutes	∞

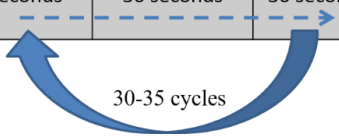

Figure 4. Conditions of PCR using Q5 polymerase.

2.2.4 Colony PCR

Colony PCR is a method for the verification of the presence of the insert after cloning. It allows to screen numerous colonies at the same time without isolating plasmids.

1	2	3	4	5	6
Initial denaturation	Denaturation	Annealing	Elongation	Final Elongation	On hold
95°C	95°C	Annealing temperature *	72°C	72°C	4°C
2 minutes	30 seconds	30 seconds	1 minutes/kb	5 minutes	∞

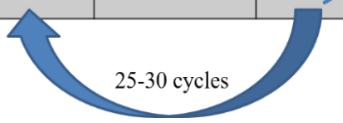

Figure 5. Conditions of PCR using pfu polymerase.

2.2.5 Agarose gel electrophoresis

Agarose gel electrophoresis enables the detection of the size of DNA following PCR amplification or restriction enzyme digestion taking the advantage of negative charged DNA and sizes of the pores within the agarose gel. 1%-2% agarose gel was prepared depending on the size of the target DNA fragment by dissolving agarose in 1X Tris-Acetic acid-EDTA (TAE). 1% (v/v) SyBr-safe was added to the mix. After cooling down, mix was poured into the reservoir in the gel tank. Wells to be loaded with DNA were formed with the help of a comb. 5 µl of Loading Dye (6x) for per 25 µl reaction was added onto the samples. Samples loaded into the wells were run on the gel at 120 V for 30-40 minutes.

2.2.6 Plasmid isolation from bacteria

Plasmid isolation from cultured bacterial cells were performed using GeneJET Plasmid Miniprep Kit of Thermo Fisher Scientific by following manufacturer's protocol. Some modifications and optional steps were also included. After washing step, columns were

left to air-dry at 70 ºC for three minutes. Instead of elution buffer, pre-heated ddH_2O was added onto the columns, and columns were waited at room temperature for 2-3 minutes. For elution, samples were centrifuged at maximum speed for 3 minutes. Concentration and purity of samples were assessed by measuring them with Nanodrop device. Purified plasmids can be stored at -20 ºC.

2.2.7 DNA extraction from agarose gel

Following PCR amplification or restriction enzyme digestion, DNA fragments were extracted from the agarose gel using GeneJET Gel Extraction Kit of Thermo Fisher Scientific by following manufacturer's protocol. Some modifications and optional steps were also included. As for plasmid isolation, after washing step, columns were left to air-dry at 70ºC for three minutes. Instead of elution buffer, pre-heated ddH_2O was added onto the columns, and columns were waited at room temperature for 2-3 minutes. For elution, samples were centrifuged at maximum speed for 3 minutes. Concentration and purity of samples were assessed by measuring them with Nanodrop device. Purified plasmids can be stored at -20 ºC.

2.3 Protein expression

2.3.1 Induction conditions

For protein expression, targeted plasmids were transformed to BL21(DE3). Cells were grown o/n at 37°C at 200 rpm and then diluted 1:100 in 10 mL fresh LB with appropriate antibiotics. At OD_{600} 0.4-0.6 cells were induced with anhydrotetracycline (aTc) or/and isopropyl β-d-1-thiogalactopyranoside (IPTG) for 24 hours at 18°C, 200

rpm. 1mM IPTG was used to induce the gene expression of the genes under the control of lac operator whereas 25 ng/mL aTc was used to control induction from.

2.3.2 Protein expression verification via SDS-PAGE and western blotting

To verify protein expression sodium dodecyl sulphate–polyacrylamide gel electrophoresis (SDS-PAGE) analysis and/or Western Blotting were performed. To perform SDS-PAGE and Western Blotting running gel consisting of 4% stacking gel and 15% separation gel was prepared. 6X SDS-loading dye was added to the samples to achieve a final concentration of 1X. Samples were incubated at heat block at 95°C for five minutes and afterwards were loaded into the SDS-PAGE running gel located inside the SDS tank properly filled with 1X SDS running buffer. Along with the stained samples 4µl of pre stained protein ladder was added. The gel used to run for 1.5 – 2.0 hours at 120V. After running the gel Coomassie Blue staining or Western Blotting was performed. To perform Coomassie Blue staining the gel was carefully removed from the SDS glass slides and placed in a container properly filled with Coomassie Blue dye. The container was placed inside the microwave for 15-40 seconds and afterwards the gel was incubated inside SDS de staining buffer and placed into the shaker for about 1.5-2.5 hours. The de staining buffer was discarded and renewed every 30 minutes. To perform Western Blotting, the gel was transferred to PDVF membrane with the Bio-RAD turbo-blot device using the standard miniblot protocol. Then the membrane was incubated into blocking solution for two hours at room temperature (RT) at shaker 250 rpm. The blocking solution consisted of 5% milk powder dissolved in TBS-T buffer. After blocking the membrane was incubated, into Anti-His goat primary antibody dissolved in TBS-T (dilution factor 1:10000), overnight at +4°C at 250 rpm. Afterwards the

membrane was washed three times with TBS-T buffer in 5,5,10-minute intervals and incubated into HRP-linked anti-goat secondary antibody dissolved in TBS-T (dilution factor 1:10000), for one hour at room temperature, 250 rpm. After the incubation the membrane was washed again similarly to the aforementioned washing procedure and the BIO-RAD ECL substrate kit was used for membrane irradiation. At the end BIO-RAD CHEMIDOC was used to capture images of the membrane.

2.3.3 SDS-PAGE/ Western Blotting sample preparation for secreted proteins

To prepare Western Blotting samples of secreted proteins Trichloroacetic Acid (TCA) protein precipitation or Acetone protein precipitation techniques were performed. For TCA precipitation the supernatant from the induced culture batch was mixed with TCA at a ration 4:1 (v/v) and stored at +4°C for 10 minutes. Then the samples were centrifuges at 14.000 rpm for five minutes and the supernatant was discarded. The pellet was washed twice with cold acetone (previously stored at -20°C) with each time following a centrifugation at max speed for 2 minutes and removal of the acetone. After washing procedure, the pellet was dried at +95°C for five minutes and at the end dissolved into 1X SDS-PAGE loading dye. For Acetone precipitation supernatant from induced samples was mixed with acetone at a ration 5:1 (v/v) and stored overnight at -20°C. The samples were centrifuged at maximum speed for 45 minutes at +4°C. Then the supernatant was discarded, and the precipitated proteins pellet was dried at +95°C for 5 minutes. Afterwards the pellet was dissolved into 1X SDS-PAGE loading dye.

2.3.4 Heat release of surface displayed nanobody

To understand if the nanobody was expressed on the surface of the bacteria via western blotting heat release was performed to the samples. To do so 5x10^8 cells were collected and suspended into 200 µl 1XPBS. The sample were then incubated at +60°C for five minutes and then centrifuged at maximum speed for another five minutes. The supernatant was collected and mixed with 6X SDS-PAGE loading dye to reach a final concentration of 1X.

2.3.5 Immunocytochemistry (ICC) visualization

Immunocytochemistry (ICC) is an immunostaining method enabling the verification expression and localization of the protein of interest within cells. A combination of antibodies is utilized to both target and label the protein of interest. While primary antibodies target the protein, secondary antibodies conjugated to fluorophores bind to the primary antibodies and intensify the signal to be visualized under fluorescence microscope. For slide preparation, a frame-shaped parafilm is heated on the heat block. The empty space is used of cell spreading, blocking, washing and immunostaining steps. Incubation steps take place on benchtop shaker for 5 minutes for efficient binding and washing. Antibodies are diluted in a buffer composed of 1% of BSA within PBST (PBS+ 0.1% Tween 20). After overnight incubation under inducing conditions, 5-10 ml of the cell culture is centrifuged at 4000 g for 15 minutes. Cell pellet is treated with 1 ml of 4% formaldehyde diluted in PBS and cell suspension is incubated at room temperature for 30 minutes. For washing step, cells are centrifuged at 1500 g for 5 minutes and resuspended in 1 ml PBS two times. Since the protein of interest is located on cell surface, steps for permeabilization is skipped and cells are spread onto the slides after fixation. 10 µl of cell suspension is pipetted onto the positively charged slide and

spread via a sterile tip. Slides are left to dry. To prevent nonspecific binding of antibodies, slides are incubated in blocking solution containing 1% of BSA within PBST (PBS+ 0.1% Tween 20) for 30 minutes. After removal of blocking solution, cells are incubated with 1:300 dilution of primary antibody for 2 hours at room temperature. Following washing in 500 µl of 1X PBS, cells are incubated with 1:500 dilution of secondary antibody at +4 ºC in a dark environment overnight. Cells are washed in PBS twice, and slides are left to air-dry. Then, one drop of mounting medium is added onto the cells in order to protect the staining for longer period of time. Parafilm frame is removed, and a cover glass is placed on each slide. Cover glass is fixed onto the slide with the help of a nail polish. At this step, slides can be either visualized under fluorescence microscope or stored at +4 ºC.

2.5 Cell culture

2.5.1 JIMT1 and MDMAB231 mammalian cell maintenance, cultivation, counting and stock preparation

Jimt1 and MDAMB231 cell lines stably transfected with green fluorescence protein (GFP) were kindly provided from Molecular Biology and Genetics Department at Bilkent University and were stored at -80°C. Both cell lines were cultivated into media containing 88% low glucose Dulbecco's Modified Eagle Medium (low glucose DMEM) without L-glutamine, 10% Fetal Bovine Serum (FBS), 1% Penicillin/ Streptomycin (Pen/Strep) antibiotic, and 1% L-glutamine. To start the first culture the stock vial was left at room temperature to defrost and was added into a 15 mL falcon filled with 13 mL freshly prepared cultivation media. Samples were centrifuged at 2500 rpm for five

minutes and then the supernatant was carefully discarded. The pellet was dissolved into 1 mL fresh cultivation media and added into a T25 flask together with 2 mL cultivation media to reach a final volume of 3 mL. The flask was incubated at 37°C, 5% CO_2. The media was changed every two days upon washing with 3mL 1X PBS. When confluency reached 80%-90% the cells where passaged. To passage the cells trypsin was used to de attach the cells from the surface upon media removal and washing with 1X PBS (1.5 mL for T25 flask). The flask was stored into the incubator for five minutes and then the solution was placed into a 15 mL falcon consisting of 13 mL fresh media. Upon centrifugation at 2500 rpm for 5 minutes the pellet was dissolve into 1 mL fresh cultivation media and 10 µL of the sample added into a PCR tube to later be diluted 1:10 with fresh media. 10 µL of the latter solution was diluted with Bromophenol Blue to a 1:1 (v/v) ratio. 10 µL of the solution were added into both sides of the counting chamber covered by a coverslip glass. The slide was observed via inverted fluorescence microscopy at 10X magnification size at bright field. All the cells located inside the big middle square (S1 and S2) boarded on four sides by three lines were counted (two sides of the square were chosen and the cells touching those borders were counted whereas the ones touching the other borders were not considered) and the total number of cells in 1 mL was determined using the following formula:

$$Total\ number\ of\ cells = 2 \times \frac{S1 + S2 + .. Sn}{n} \times\ 10^4 \times dilution\ factor$$

To prepare stock solution one million cells were stored at 10% DMSO. The cell stock vial was placed in an isopropanol chamber and stored at -80°C overnight. The following day the vial was transferred into the nitrogen tank and stored there for further usage.

2.5.2 MTT assay

MTT (3-(4, 5-dimethylthiazolyl-2)-2, 5-diphenyltetrazolium bromide) assay is a colorimetric viability assay. Viable cells convert MTT into a purple color whereas the dead cells cannot mediate the color change. The samples absorbance levels are measured at a 570 nm wavelength using a spectrophotometer (41).

CHAPTER 3

RESULTS AND DISCUSSION

3.1 Expression of the nanobody at the surface of *E. coli*

3.1.1 Selection of the nanobody and the mammalian cells to be targeted

In order for our bacteria to target mammalian breast cancer cells 2Rs15d nanobody, which binds to HER2 receptor (42), was selected. Nanobodies are fully functional antibodies, but they lack the light chains that are found in the antibodies and consist only the heavy chains. They are naturally produced by Camelids and are smaller in size and more resistant to heat compared to antibodies (43). In our study Jimt1 breast cancer cells are used. Jimt1 cells overexpress HER2 receptor and therefore were thought as a proper target for our study. Jimt1 mammalian cells were kindly provided by MBG department at Bilkent University whereas the gene sequence of 2Rs15d nanobody was obtained from Genewiz.

3.1.2 Ag43 cell surface expression system.

In order to express the nanobody at the surface of *E. coli* Ag43 autotransporter protein was used. This protein uses Type V secretion pathway to secrete the protein of interest into the outer surface of *E. coli*. It consists of an N-terminal signal sequence (pelB), a passenger domain as well as an alpha and beta subunit. The protein of interest is cloned alongside the N-terminal signal sequence. The secretion system is a two-step secretion pathway where first the protein is secreted into the periplasm via SecYEG translocon

and then beta barrels are formed and inserted into the outer membrane of E. coli and the protein of interest is expresses at the surface of *E. coli* (44).

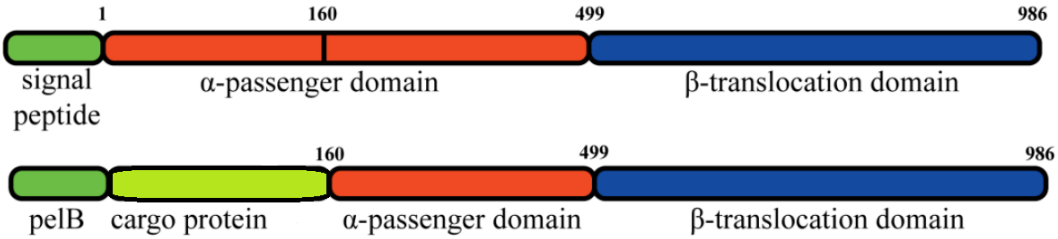

Figure 6. Schematic representation of Ag43 autotranspoter protein domains. Picture adapted from Seker et. al (44).

3.1.3 Cloning of pET22b T7-LacO pelb 2Rs15d Ag43 AmpR

The 2Rs15d nanobody was cloned downstream T7 LacO promoter into a pET22b vector. The backbone was obtained from pET22b Ag43 160N 6h sfGFP AmpR plasmid that was provided from Recep Erdem Ahan, a member of our lab. It consisted of Ag43 secretion cassette which would mediate the expression of the nanobody at the surface of *E. coli.*

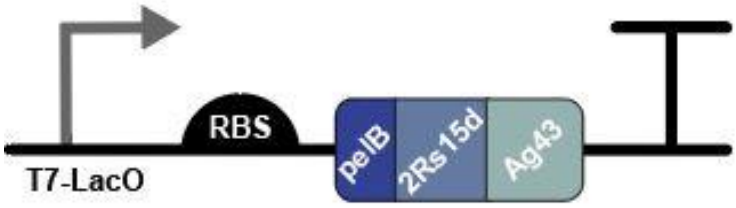

Figure 7. Schematic representation of T7-LacO pelb 2Rs15d Ag43 construct. Moreover, a signal peptide (pelB) mediated the localization of the cargo into the periplasmic space.

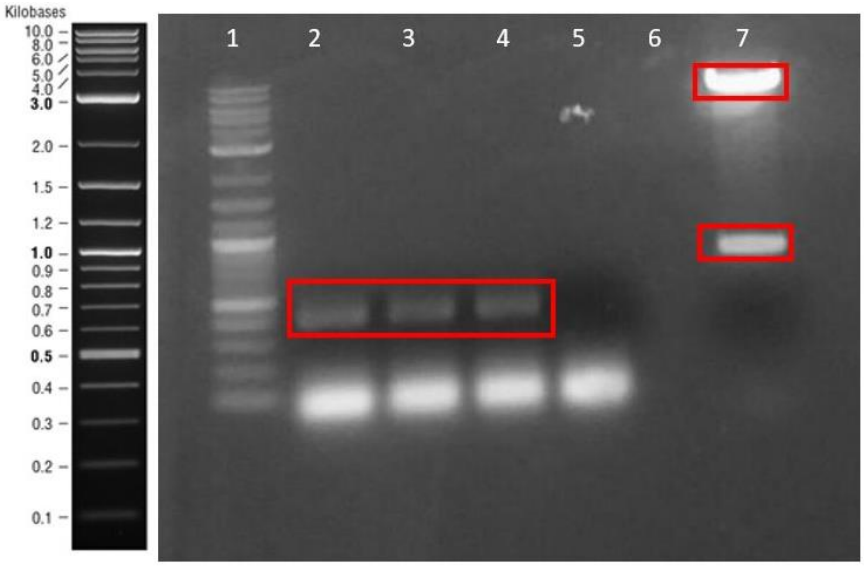

Figure 8. PCR rection to amplify the nanobody gene from the ordered gene fragment and restriction digestion reaction of pET22b Ag43 160N sfGFP AmpR to obtain the backbone. Lanes: (1) 2log DNA ladder, (2-4) PCR amplification reactions for 2Rs15d, (5) PCR reaction negative control, (6) Restriction digestion reaction negative control, (7) Restriction digestion reaction. Expected sizes are ≈ 404 bp for the PCR product whereas for the restriction digestion reaction expected sizes are ≈796 bp and ≈8 kb. After gel extraction was performed, the parts were assembled via Gibson Assembly. The end product of the reaction was transformed in E. coli DH5 α and two colonies were sent for sequencing. The correct plasmid was later on transferred into *E. coli* BL21 (DE3).

3.1.4 Binding assay to test the binding of our bacteria to Jimt1 mammalian cells

In order to test if bacteria were binding to Jimt1 mammalian cells a binding assay was performed. Jimt1 mammalian cells used in this study are stably transformed with GFP

and under fluorescence microscope they appear as green. To determine the localization of our bacteria pZA mproD RFP CmR plasmid, which mediates the expression of red fluorescence protein, was transformed into the same bacteria. The double transformed bacteria were properly induced with 1 mM PTG as explained in the materials and methods section. The bacteria were then centrifuged at 8000 rpm for 10 minutes and the media was discarded. The pellet was dissolved in 1XPBS under sterile conditions.

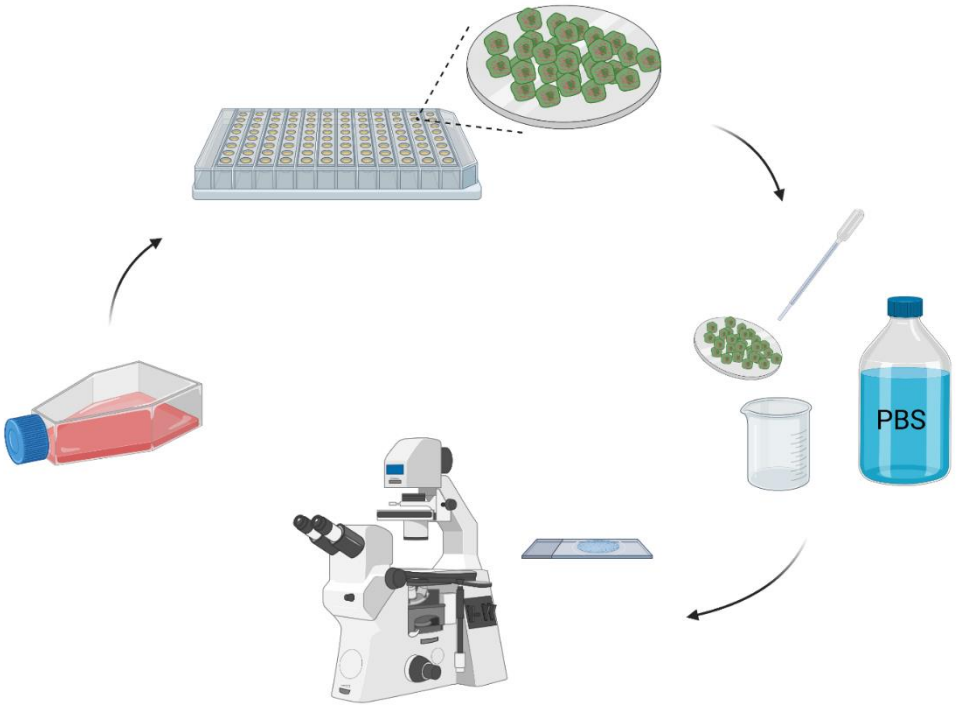

Figure 9. Schematic representation of the performed binding assay.

Meanwhile Jimt1 mammalian breast cancer cells were cultured in a T25 cm^2 flask. When confluency reached a level of 80-90% the cells were passaged and 10^5 mammalian cell were added into each well of a 24 well plate, in a media lacking FBS and antibiotic. Each well consisted of a glass slide at the bottom. The growth of the mammalian cells and the induction of the bacteria were arranged to be completed at the

same time. Afterwards 10^7 bacteria were counted and added to each well consisting of the mammalian cells. The plate was then incubated for 1 hour at 37°C and afterwards the glass slides were taken and washed three times with 1xPBS. After washing microscope slides were prepared and pictures were taken under fluorescence microscope.

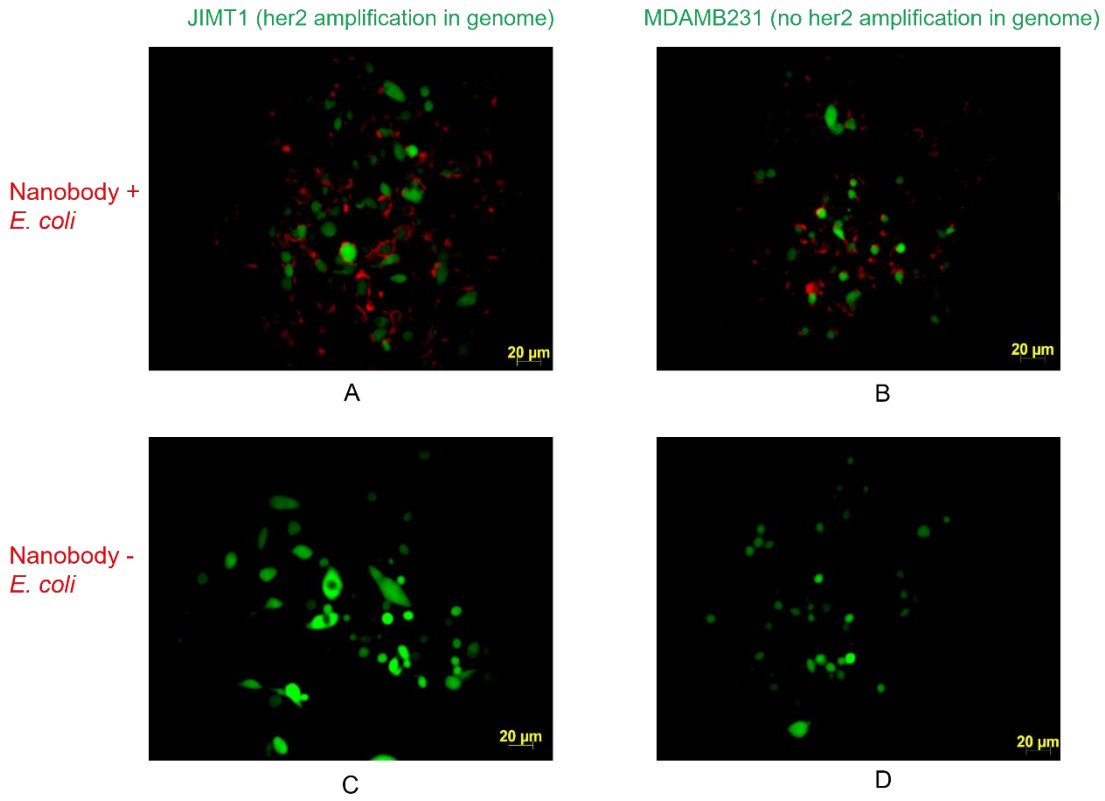

Figure 10. Inverted fluorescence pictures taken after coculturing bacteria and mammalian cells for two hours. A) *E. coli* BL21 (DE3) expressing 2Rs15d nanobody and Jimt1 after one hour of incubation. B) *E. coli* BL21 (DE3) expressing 2Rs15d nanobody and MDA MB 231 after one hour of incubation. C) *E. coli* BL21 (DE3) and Jimt1 after one hours of incubation. D) *E. coli* BL21 (DE3) and MDA MB 231 after one hour of incubation. Scale bar 20 µL for all pictures.

Bacteria appear in red because they have been transformed with pZA mproD RFP, whereas Jimt1 and MDA MB 231 breast cancer cells appear in green since they have been stably transfected with GFP expressing plasmid. The microscope data show that our engineered bacteria bind to Jimt1 breast cancer cells. Moreover, we see that there is binding also to the MDA MB 231 cancer cells. Even though these cells do not express HER2 receptor at the same levels as Jimt1 breast cancer cells there is still some expression which leads to binding affinity of our bacteria. Regarding the *E. coli* expressing no nanobody there is no binding and the bacteria have been washed away.

3.2 Verification of the expression of HlyE at the surface of *E. coli* BL21 (DE3)

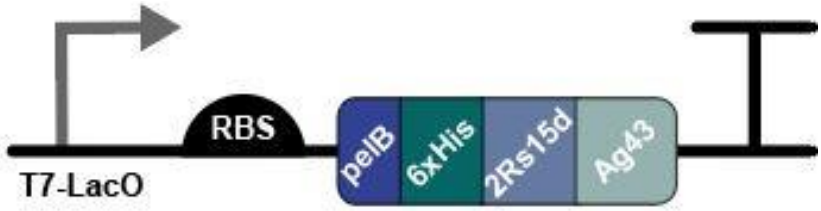

Figure 11. The schematic representation of T7-LacO pelb 6xHis 2Rs15d Ag43 construct.

The 2Rs15d nanobody was cloned into an identical backbone which consisted of a histidine tag to verify the expression of the nanobody at the surface of *E. coli* BL21 (DE3) via Western blotting and Immunocytochemistry. To perform the expression analysis cells were properly grown and then induced with 1 mM IPTG as explained in the materials and methods section. Afterwards western blotting and immunocytochemistry samples were prepared. All the western blotting samples consisted of the supernatants and heat release was performed as explained in the

materials and methods section. The immunocytochemistry fluorescence pictures, and western blotting data are shown below.

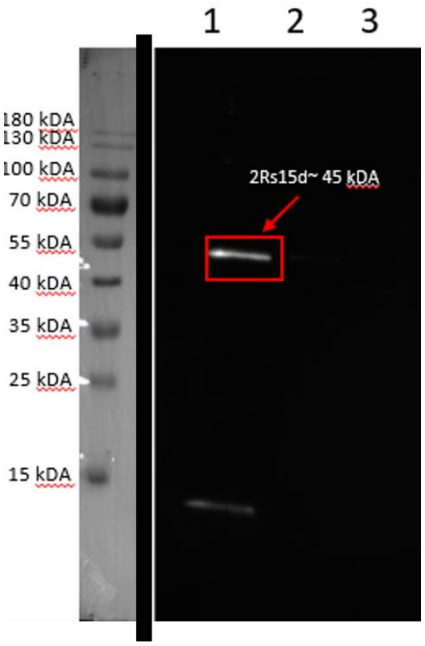

Figure 12. Western blotting picture to prove 2Rs15d nanobody expression at the surface of *E. coli*. Lanes: (1) *E. coli* BL21 (DE3) pET22b T7-LacO 6xHis pelb 2Rs15d Ag43 AmpR induced with 1 mM IPTG, (2) *E. coli* BL21 (DE3) pET22b T7-LacO 6xHis pelb 2Rs15d Ag43 AmpR uninduced, (3) *E. coli* BL21 (DE3). Expected size of fusion of nanobody and alpha subunit ≈49 kDA. All samples consist of the supernatants. The lower band at the first lane corresponds to 2Rs15d nanobody ≈ 13 kDa.

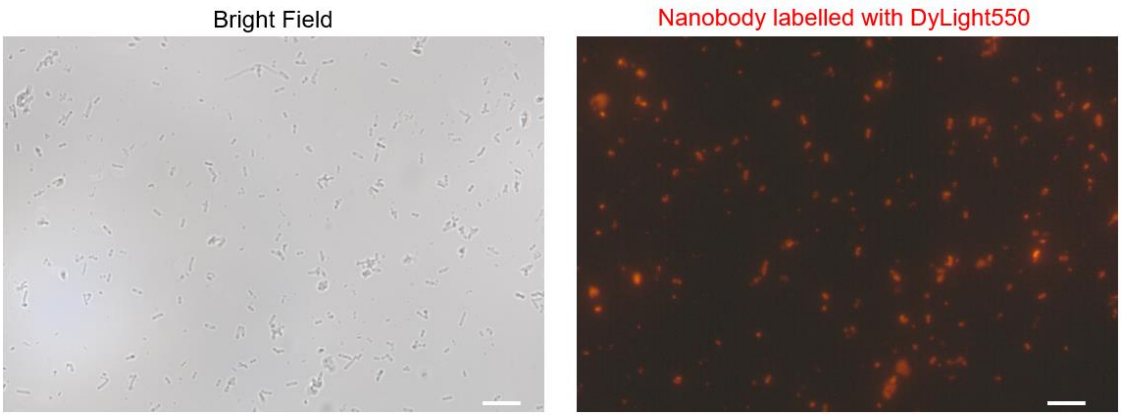

Figure 13. Pictures taken under fluorescence microscope after immunocytochemistry sample preparation from *E. coli* BL21 (DE3) pET22b T7-LacO 6xHis pelb 2Rs15d Ag43 AmpR. (I) Bright Field, (2) Fluorescent Picture. Scale bar is 10 μm.

Via western blotting data and immunocytochemistry, it was proven that the nanobody is expressed at the surface of *E. coli*.

3.3 Production of HlyE intracellularly

3.3.1 Cloning of HlyE to pET22b GST 6xHis AmpR vector

In order for us to prove that HlyE toxin can kill Jimt1 mammalian cells we decided to produce the toxin intracellularly.

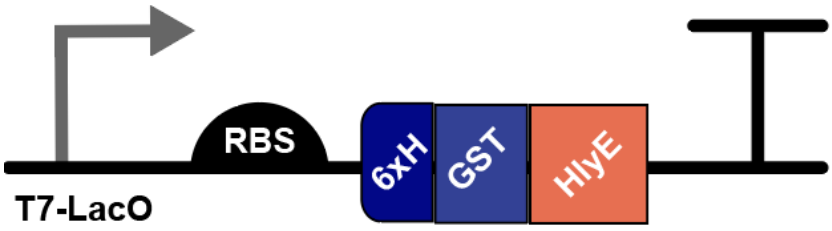

Figure 14. Schematic representation of T7-LacO GST HlyE 6xHis construct.

HlyE gene was cloned into pET22b 6his GST AmpR vector under T7 LacO promoter. A GST tag was also present as well as a histidine tag so that we would have no problems with purification steps. GST tag also improves the solubility of the protein. pET22b 6his GST AmpR backbone was provided from Recep Erdem Ahan. HlyE gene was amplified via PCR using pZA YebF HylE 6xhis AmpR vector as template, whereas the backbone was obtained from the digestion of pET22b T7 LacO GST TEV 6xhis AmpR vector with BamH1 and Xho1 restrictions enzymes. The digestion reaction was formed and placed at 37°C for 2.5 hours. The samples were later on run on gel electrophoresis. The results are shown in the following pictures.

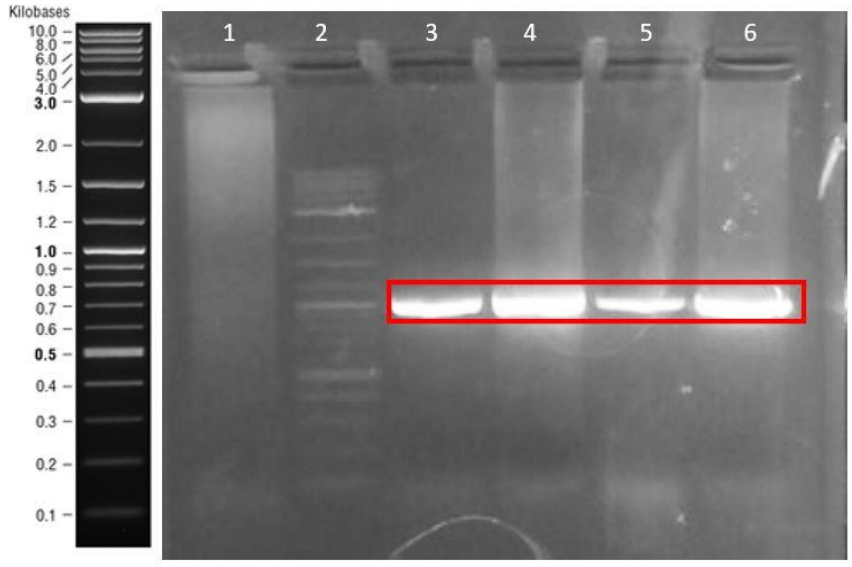

Figure 15. PCR amplification of HlyE gene from pZA pL-tetO HlyE 6xhis AmpR vector. Lanes: (1) Negative control, (2) 2log DNA ladder, (3-4) PCR reactions. Expected side ≈ 909 bp.

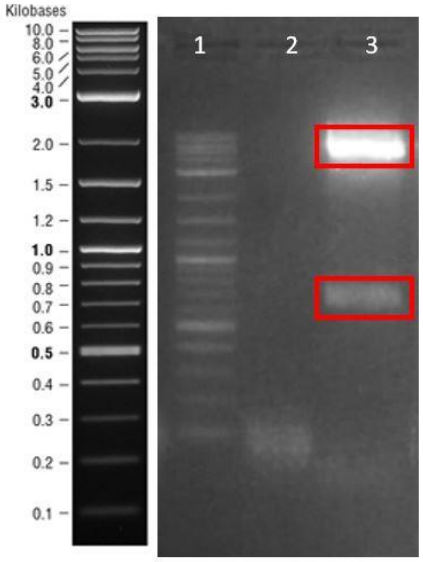

Figure 16. Restriction digestion reaction of pET22b T7 lacO GST TEV 6xhis AmpR vector with Bamh1 and Xho1 restriction enzymes. Lane: (1) 2log DNA ladder, (2) Negative Control, (3) Restriction digestion reaction. Expected sizes ≈ 6 kb and 732 bp.

After running the gels, the required fragments were cut, and gel extraction was performed. After that, Gibson assembly was done, and the product was transformed in *E. coli* PRO DH5α. The other day three colonies were chosen from the transformation plate and were inoculated into 10 mL liquid broth media with appropriate antibiotic. The cells were grown overnight and afterwards diluted 1:100 in LB and placed in 37°C till OD_{600} reached a value of 0,4-0,6. Then the cells were induced with 1 mM IPTG overnight at 18°C. The following day SDS-PAGE was performed for all the colonies as shown in the figure. The colony with the correct size was sent for verification via sanger sequencing and the work was continued.

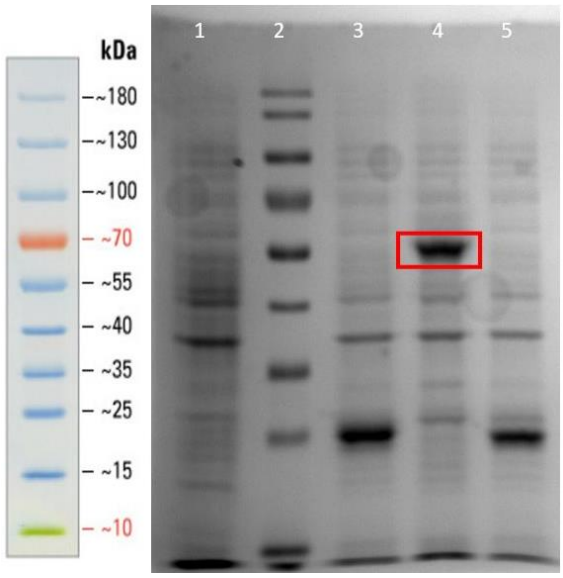

Figure 17. SDS-PAGE of the colonies transformed with pET22b T7 lacO 2Rs15d Ag43 AmpR Gibsson Assembly product after being induced with 1mM IPTG overnight. Lanes: (1) BL21 DE3 cell lysate, (2) Page Ruler protein ladder, (3-5) the induced colonies. Predicted size of the protein using Expasy program is ≈ 59 kDa.

3.3.2 Purification of HlyE

After doing the transformation the cells were induced with 1 mM IPTG and the protein was purified using histidine tag columns and the eluted samples were run in SDS-PAGE. As shown in the figure below, the protein was concentrated on second and third elution tubes. After purifying the protein, we did buffer exchange with 1xPBS because the protein was dissolved in imidazole, which is toxic to mammalian cells. After doing buffer exchange we continued with testing our toxin into mammalian cells.

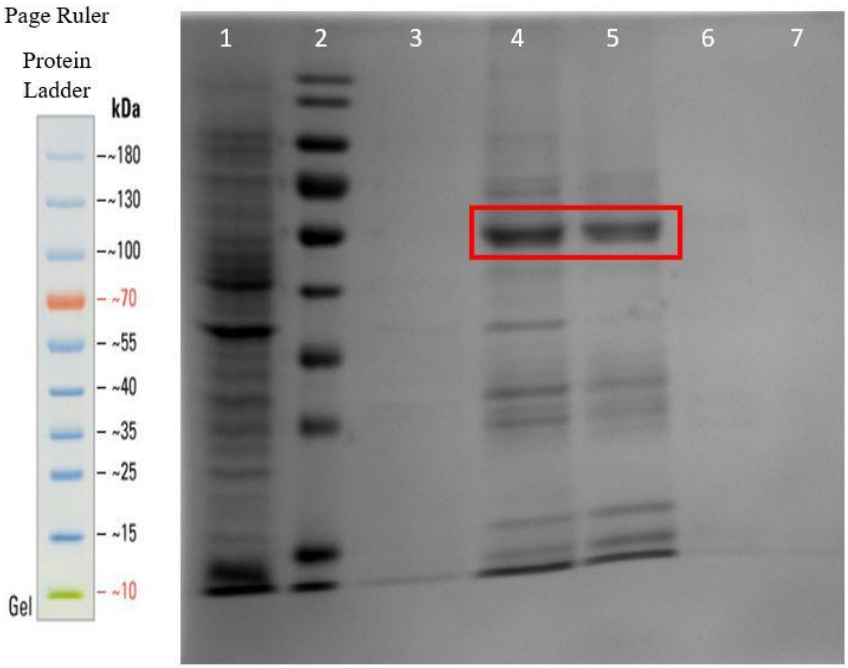

Figure 18. SDS-PAGE of eluted samples from the purification process of HlyE GST Histidine tag protein. Lanes: (1) BL21 DE3 cell Lysate- Negative control, (2) Page Ruler-Protein ladder, (3-7) Eluted samples. Expected size of the protein ≈59 kDa.

3.3.3 Testing of HlyE onto mammalian cells

After purifying hemolysin E, we had to test the toxin into Jimt1 mammalian cells. First a Jimt1 cell stock was open, and cells were plated into a T25 cm^2 flask. The media of the cells was changed every other day and when confluency reached a level of 80-90% the cells were removed via trypsin and counted as explained in the materials and methods section. After counting, 10^4 Jimt1 cells were dissolved in 100 µL growth media and placed into each well in a 96 well plate.

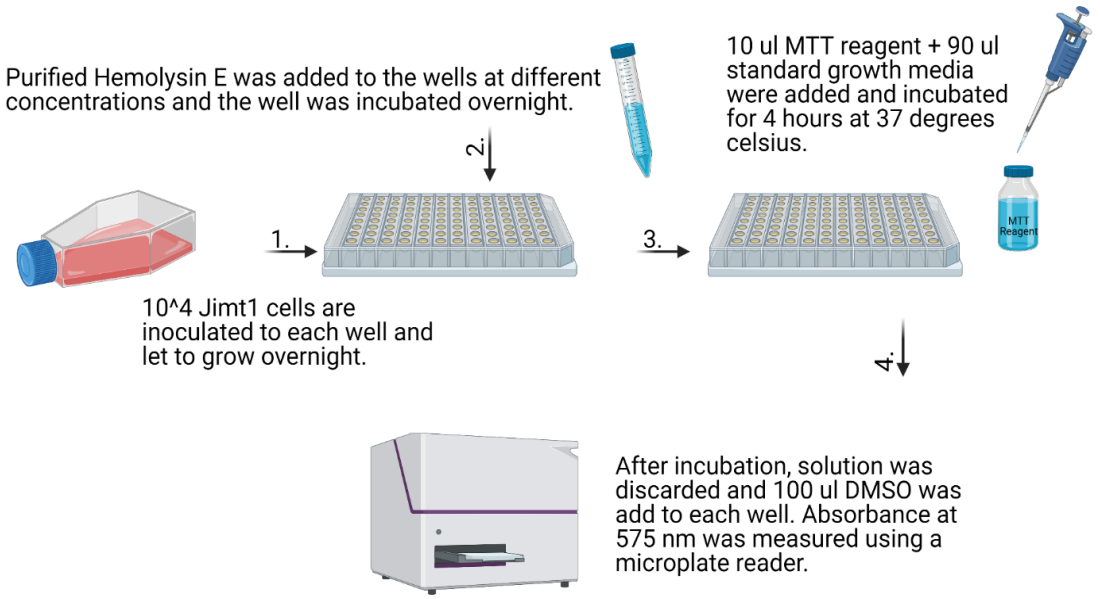

Figure 19. Schematic representation of toxicity assay design.

The cells were grown overnight and after that the purified toxin dissolved in PBS was added at different concentrations volumes: 10 µL, 30 µL, 50 µL, 100 µL. Controls with the same volumes of PBS were prepared as well. There were three replicas for each sample. The 96 well plate was placed at the incubator overnight and the other day MTT assay was performed. The absorbance measurements at OD_{570} are shown in the following table.

Sample Name	OD_{570} Measurement for Replicas (1-3)		
10 µL HlyE	0,399	0,344	0,343
10 µL 1xPBS	0,680	0,765	0,648
30 µL HlyE	0,401	0,325	0,320
30 µL 1xPBS	0,440	0,551	0,589
50 µL HlyE	0,416	0,134	0,208
50 µL 1xPBS	0,483	0,650	0,517
100 µL HlyE	0,061	0,065	0,079
100 µL 1xPBS	0,425	0,413	0,397

Table 1. OD_{570nm} measurements for toxicity assay experiment.

After doing the measurements statistical analysis were performed and the results were as following.

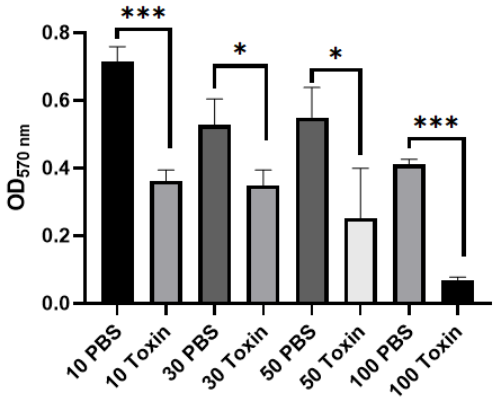

Figure 20. Unpaired t test statistical analysis was performed to compare cell viability in different PBS and toxin concentrations. Based on unpaired t test significant difference with a value of $p \leq 0.05$, $p \leq 0.01$, $p \leq 0.001$ are shown with "*", "**", "***" respectively.

According to the obtained data we conclude that our toxin is working properly, and it can kill Jimt1 breast cancer cells. Regarding the results of the samples with 30 µL, 50 µL toxin and PBS it can be attributed to experimental errors causing standard deviation.

3.4 Secreting Hemolysin E in the extracellular space of *E. coli* BL21 (DE3)

3.4.1 Hemolysin E to kill breast cancer cells

After being able to show that our bacteria binds to Jimt1 mammalian cells we decided to engineer *E. coli* to secrete a therapeutic into the cancer site. The selected therapeutic was toxin Hemolysin E. It is a rod-shaped molecule that is naturally produced in *Salmonella* typhi, *Shigella* flexeri, *E. coli* K12 etc. It has no effect on the bacterial cell membranes from and it is hypothesized that the presence of cholesterol in the target membranes stimulates the lytic activity of the protein (45). This toxin is not produced by *E. coli* PRO DH5α and *E. coli* BL21 (DE3) so we had to amplify the gene from the genome of *E. coli* K12 strain.

3.4.2 Secreting Hemolysin E via YebF secretion system

After selecting the toxin, we had to decide on the secretion system that we would implement. Different studies had shown the efficacy of YebF system to secrete different proteins in the extracellular space of *E. coli* (46, 47, 48), therefore we decided to implement this system for the secretion of Hemolysin E. This secretion system involves two steps: in the first step the protein is localized in the periplasmic space via the sec- or tat- system and in the second step the protein is secreted to the extracellular space via the help of OmpF, OmpC and OmpX outer membrane proteins (49).

3.4.3 Cloning of pZA pL-tetO YebF HlyE 6xhis AmpR

The backbone for building up this plasmid was obtained from Recep Erdem Ahan whereas the hemolysin gene was amplified from the genome of *E. coli* K12 via PCR.

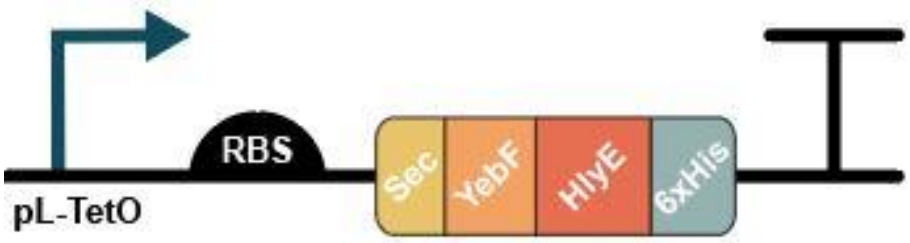

Figure 21. Schematic representation of pL-tetO YebF HlyE 6xHis construct.

To amplify the toxin JO5 and JO6 primers were used, whereas for obtaining of the backbone plasmid obtained from Recep Erdem Ahan was cut with BamH1 and Afl2. The gel electrophoresis data are shown in the following pictures.

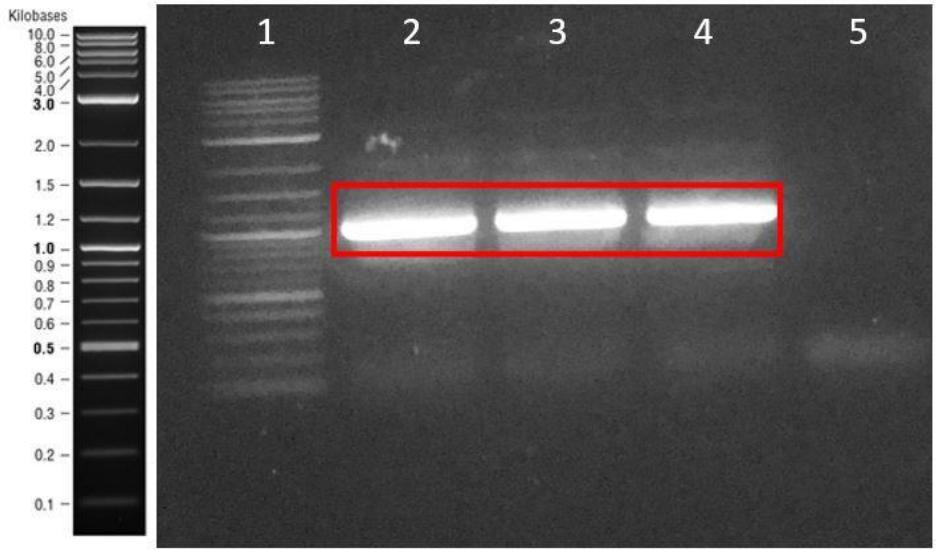

Figure 22. PCR to amplify HlyE gene from *E. coli* K12 genome. Expected size of the product is ≈ 909 bp. Lanes: (1) 2Log DNA ladder, (2-4) PCR reactions, (5) Negative control.

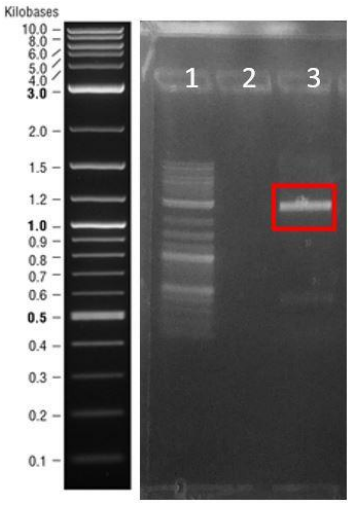

Figure 23. Digestion rection of plasmid REA64. Expected size of the product is ≈ 3000 bp and the byproduct ≈400 bp. Lanes: (1) 2Log DNA ladder, (2) Negative control, (3) Digestion reaction.

Afterwards Gibson assembly was performed, and the product was chemically transformed to *E. coli* PRO DH5α. The other day colonies from the plates were chosen and colony PCR was performed to choose the correct colonies to send for sequencing. The gel electrophoresis data is shown below.

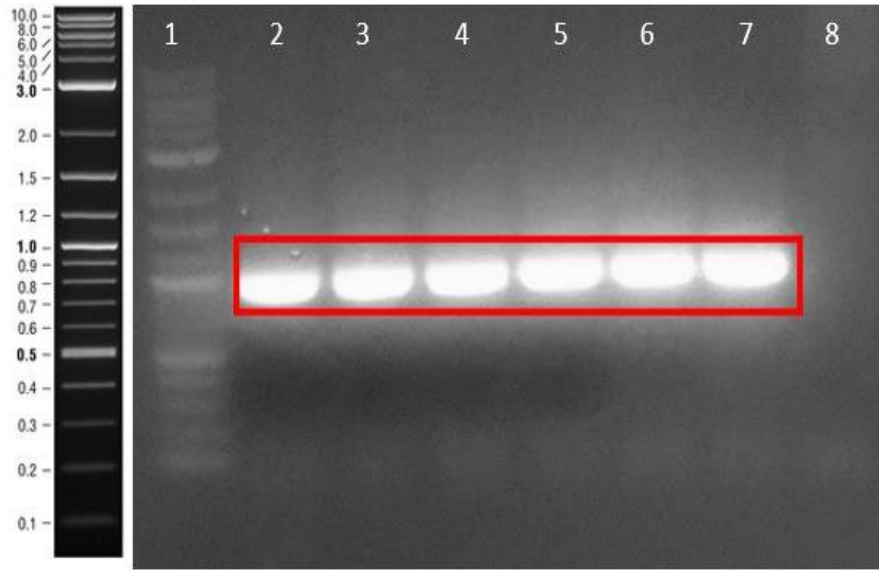

Figure 24. Colony PCR to check our cloning. Expected size of the product is ≈ 1 kb. Lanes: (1) 2Log DNA ladder, (2-7) Selected colonies PCR product, (8) Negative control.

Two colonies where chosen and isolated plasmids were sent for sequencing. After sequencing verification, the plasmid was chemically transformed to *E. coli* BL21 (DE3). After transformation the cells were induced with aTc overnight as explained in the materials and methods section. Afterwards western blotting was performed to check if our protein was produced.

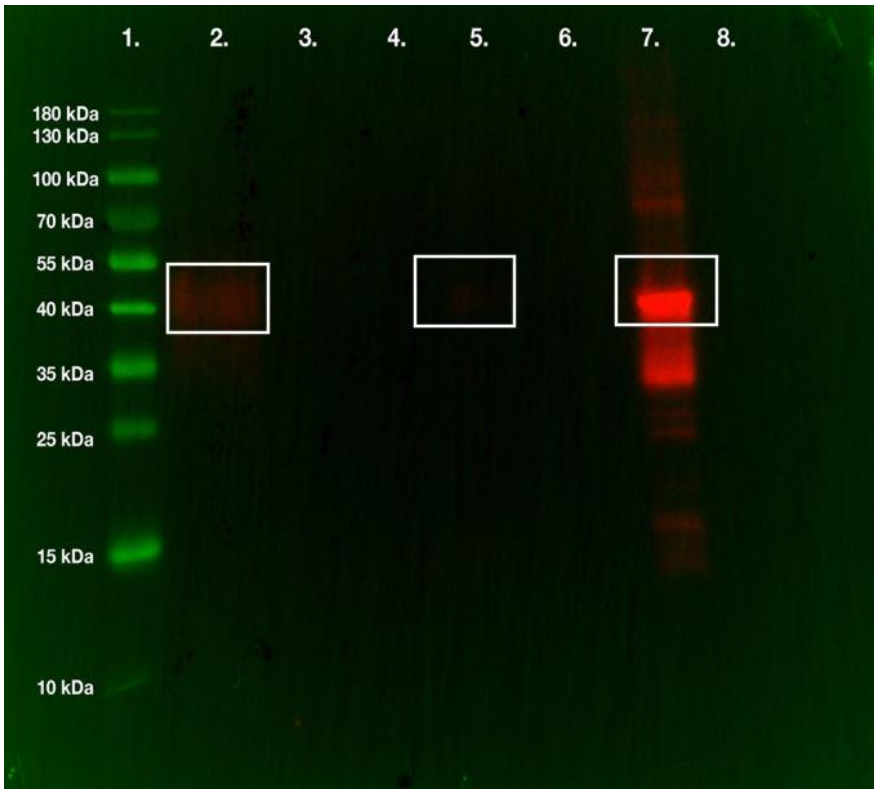

Figure 25. Western Blotting data to check expression of HlyE protein after induction with aTc. Lanes: (1) Page Ruler Protein Ladder, (2) *E. coli* DH5α HlyE supernatant (1 mL), (3) *E. coli* DH5α supernatant (1 mL), (4) Empty, (5) *E. coli* DH5α HlyE

supernatant (200 µL), (6) *E. coli* DH5α supernatant (200 µL), (7) *E. coli* DH5α HlyE whole cell, (8) *E. coli* DH5α whole cell. Expected size of fusion protein HlyE YebF≈ 48 kDa as calculated via Expasy.

The supernatant samples where concentrated via Acetone Precipitation technique to obtain better bands. Using this construct, we were able to observe toxin secretion to the surface of *E. coli*. The protein secretion however appears to be at low levels at the extracellular space which raises the necessity for improvement. Moreover, our end goal is to transform both nanobody construct and toxin construct in *E. coli* BL21 (DE3). Since both these plasmids have ampicillin resistance, and the fact that pZA pL-tetO YebF HlyE 6xhis AmpR construct would be constitutively active in *E. coli* BL21 (DE3) due to lack of tetR gene we decided to design a new construct.

3.4.4 Cloning of pET22b 6xHis HlyE TEV-Linker TEV Protease Ag43 AmpR

After testing the YebF system in *E. coli* PRO DH5α cells we decided to try another system which we called self- cleavage system. This system could be used at *E. coli* BL21 (DE3) cells as well.

Figure 26. Schematic representation of pET22b 6xHis HlyE Ag43160N TEV vector. Here we hypothesized that the protein would be expressed at the surface of *E. coli* via Ag43 system. The TEV protease which would also be expressed on the surface would cut TEV linker and release the toxin in the outer surface of *E. coli.*

To do the cloning three different PCR were performed. Linker TEV-TEV Protease were cloned first from pET22b Ag43 160N 6h TEV sfGFP via primers pREA24 and MKL2. Backbone was obtained from pET22b Ag43 160N 6h TEV sfGFP via primers pzA Ag43 atc FWD and pzA Ag43 atc REV. Lastly HlyE gene was obtained via amplification using primers JO11 and JO9. The gel electrophoresis pictures for each PCR reaction are shown below.

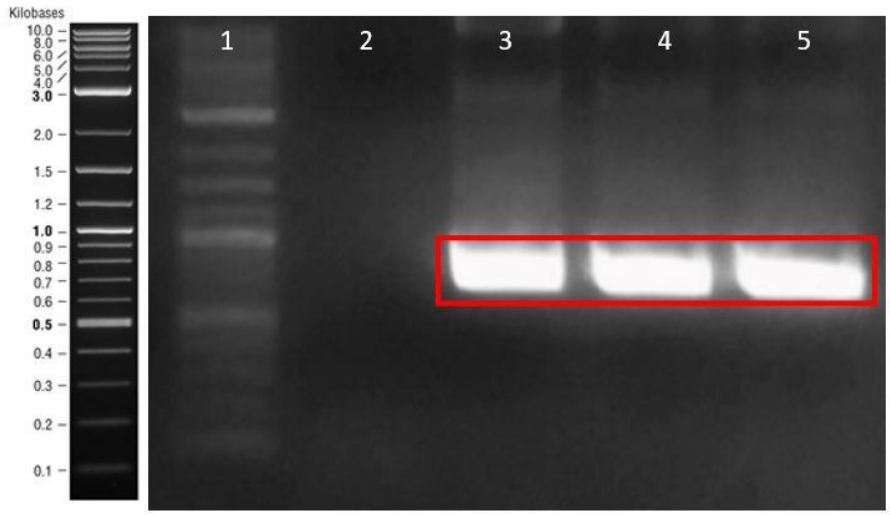

Figure 27. Gel electrophoresis picture, PCR amplification of Linker TEV- TEV Protease insert. Template DNA is pET22b Ag43 160N 6h TEV sfGFP. pREA24 and MKL2 primers are used. Expected product size ≈794 bp. Lanes: (1) 2Log DNA ladder, (2) Negative control, (3-5) PCR products.

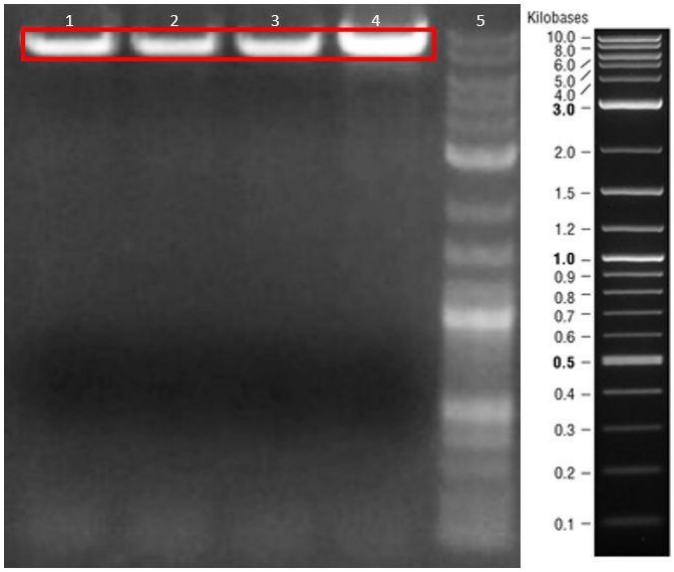

Figure 28. Gel electrophoresis picture, PCR amplification of the backbone. Template DNA pET22b Ag43 160N 6h TEV sfGFP. pzA Ag43 atc FWD and pzA Ag43 atc REV primers are used. Expected product size ≈7962 bp. Lanes: (1-4) PCR products, (5) 2Log DNA ladder.

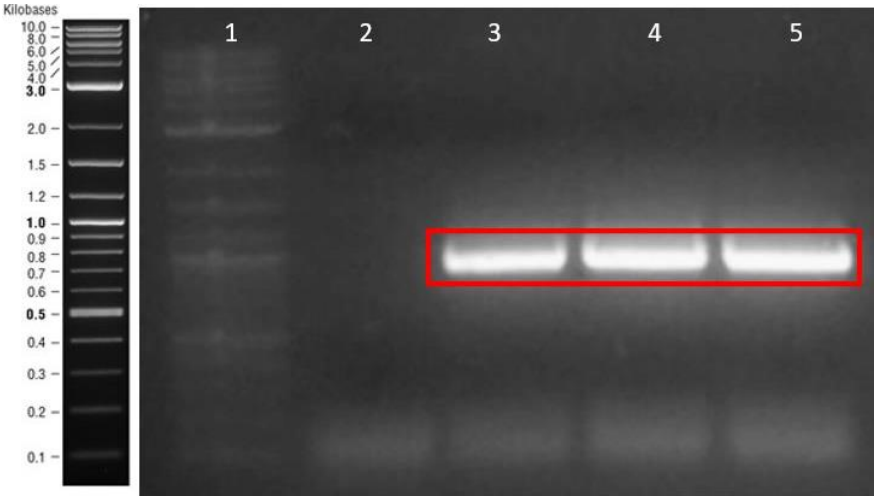

Figure 29. Gel electrophoresis picture, PCR amplification of Hemolysin E gene. Template DNA is pZA HlyE YebF. JO9 and JO11 primers are used. Expected product size ≈969 bp. Lanes: (1) 2Log DNA ladder, (2) Negative control, (1-4) PCR products.

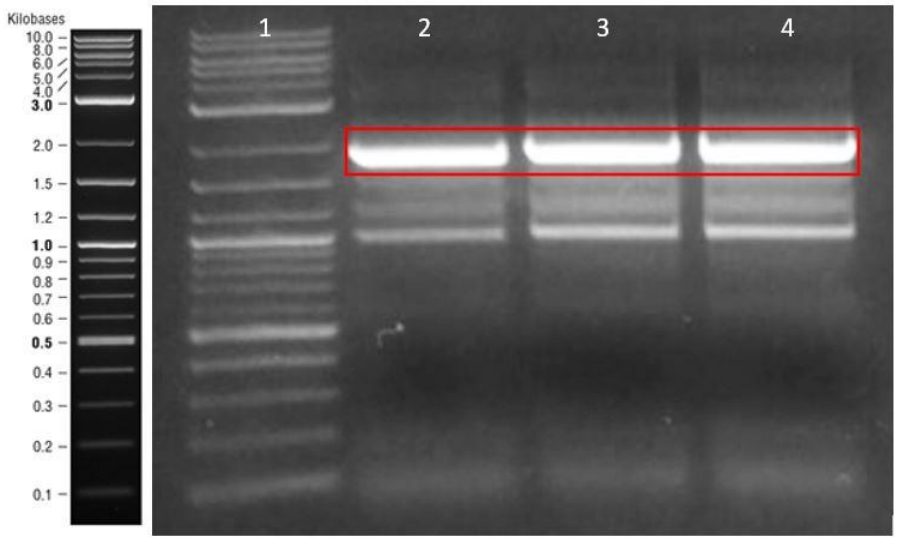

Figure 30. Gel electrophoresis picture, Two- Template PCR using the products from the Linker TEV-TEV Protease PCR and HlyE PCR. Thermal Cycler was run for 10 cycles without primers at 76°C, then MKL2 and JO9 primers was added, and Thermal Cycler was run again at 77°C for 30 cycles. Expected size is ≈ 1733 bp. Lanes: (1) 2Log DNA ladder, (2-4) PCR products.

After doing the PCR reactions the PCR products from Two-Template PCR and Backbone amplification were used in the Gibson Assembly reaction. The reason why we did Two-Template PCR was to decrease the number of DNA inserts that were going to be used for Gibson Assembly. By doing so the efficacy of the Gibson Assembly reaction is increased. After preparing the reaction the end product was chemically transformed into *E. coli* PRO DH5α. The following day appropriate colonies were chosen, and digestion reaction was performed to check if our cloning was successful. For digestion reaction EcoRV and BamH1 were used and in the case of a successful cloning 7,6 kb;

1,4kb and 700 bp bands were to be observed. Gel electrophoresis was performed using the digestion reaction products and the band sizes were observed as expected.

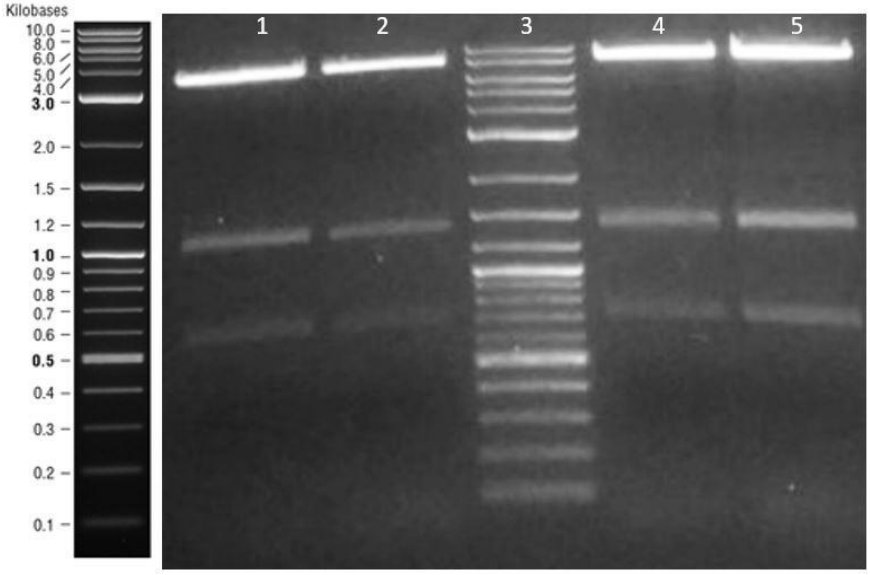

Figure 31. Gel electrophoresis of digestion reactions products. Transformed colonies were chosen and plasmid isolation was done for four of them. The plasmids were cut with EcoRV and BamH1 restriction enzymes. Expected bands ≈7,6 kb; 1,4kb and 700 bp. Lanes: (1,2 & 4,5) 4 different colonies, (3) 2Log DNA ladder.

3.4.5 Verification of HlyE secretion via pET22b 6xHis HlyE TEV-Linker TEV Protease Ag43 AmpR construct

After verification via digestion two samples were sent for sequencing and the correct colony was selected. Plasmid was chemically transformed to *E. coli* BL21 (DE3). The cell was properly induced with 1 mM IPTG and then SDS-PAGE and Western Blotting analysis were performed to control the expression of hemolysin E using this system.

Both SDS-PAGE analysis and western blotting showed almost no expression of the protein except of the cases when we overexposed the western image in which case there appeared to be very low levels of protein expression.

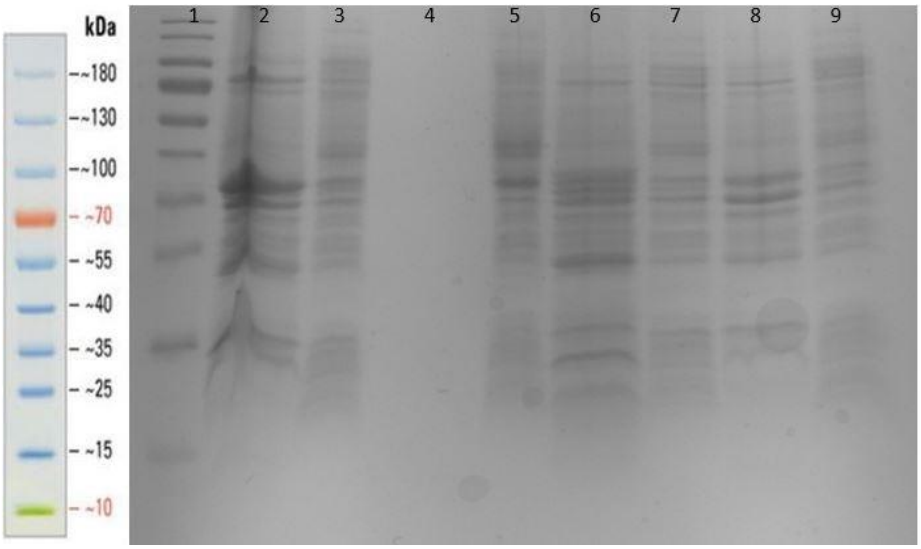

Figure 32. SDS-PAGE of the samples obtained from the new construct induced at different temperatures for different times respectively. Lanes: (1) Page Ruler Protein Ladder, (2) *E. coli* BL21 (DE3) self-cleavage supernatant (induced at 37°C), (3) *E. coli* BL21 (DE3) self-cleavage whole cell (induced at 37°C), (4) *E. coli* BL21 (DE3) supernatant, (5) *E. coli* BL21 (DE3) whole cell, (6) *E. coli* BL21 (DE3) self-cleavage supernatant (induced at 30°C), (7) *E. coli* BL21 (DE3) self-cleavage whole cell (induced at 30°C), (8) *E. coli* BL21 (DE3) self-cleavage supernatant (induced at 18°C), (9) *E. coli* BL21 (DE3) self-cleavage whole cell (induced at 18°C)

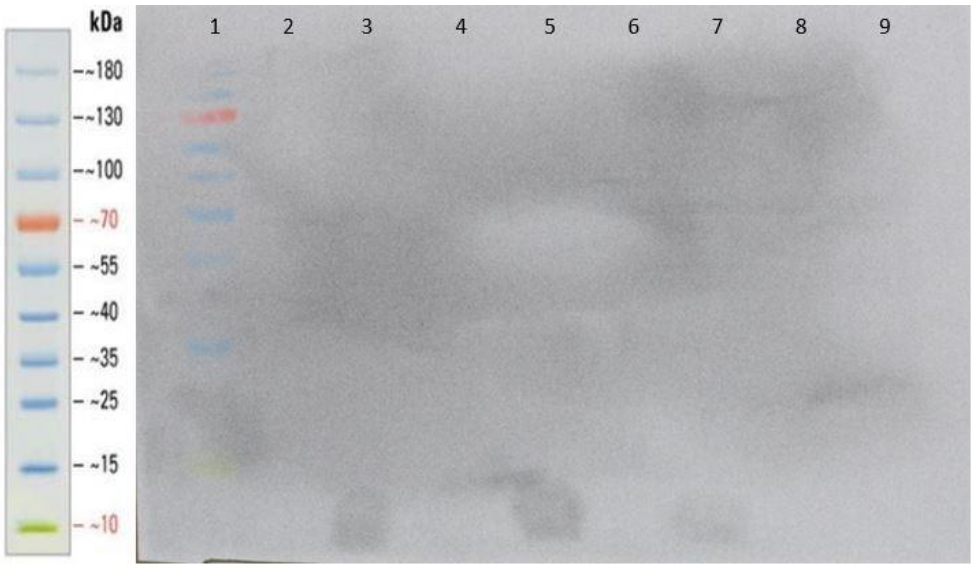

Figure 33. SDS-PAGE of the samples obtained from the new construct induced at different temperatures for different times respectively. Lanes: (1) Page Ruler Protein Ladder, (2) *E. coli* BL21 (DE3) self-cleavage supernatant (induced at 37°C), (3) *E. coli* BL21 (DE3) self-cleavage whole cell (induced at 37°C), (4) *E. coli* BL21 (DE3) supernatant, (5) *E. coli* BL21 (DE3) whole cell, (6) *E. coli* BL21 (DE3) self-cleavage supernatant (induced at 30°C), (7) *E. coli* BL21 (DE3) self-cleavage whole cell (induced at 30°C), (8) *E. coli* BL21 (DE3) self-cleavage supernatant (induced at 18°C), (9) *E. coli* BL21 (DE3) self-cleavage whole cell (induced at 18°C)

All the supernatant samples were concentrated via TCA precipitation technique. No expression of the protein was observed using self-cleavage construct. We hypothesize that due to the high number of elements in the construct misfolding of the protein is happening and therefore the protein is degraded. We decided not to use this construct as a secretion tool and continued with the following construct design.

3.4.6 Cloning of pZA native pTetO HlyE Yebf 6xHis CmR vector

At the end we decided to use pTetO native promoter which is a bidirectional promoter. Hence, we would mediate the expression of our targeted protein and TetR so that we could use this construct in *E. coli* BL21 (DE3) in an inducible form. In this system we decided to use YebF secretion system in order to release our toxin to the extracellular environment.

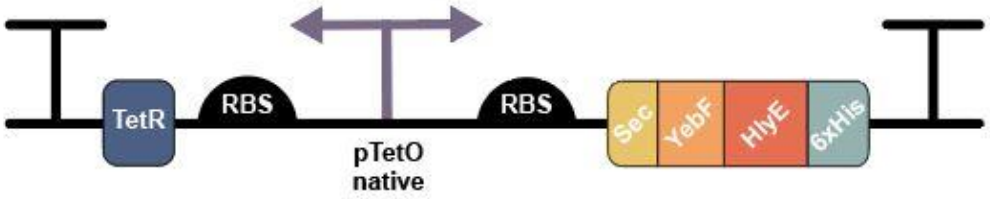

Figure 34. Schematic representation of native pTetO Yebf HlyE 6xHis construct.
The backbone was taken from pZa HlyE YebF CmR vector. Hemolysin E was amplified from the same vector.

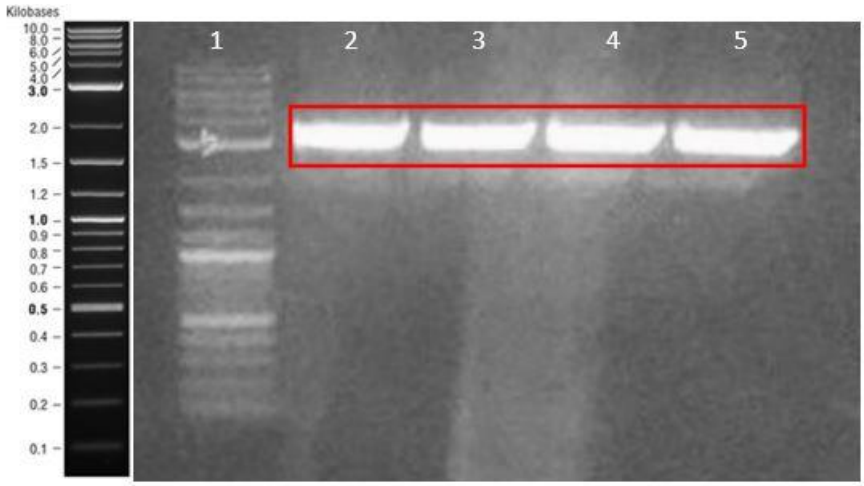

Figure 35. Gel Electrophoresis of PCR products performed for the amplification of the backbone. pREA29 and pREA78 were used as primers and the template was pZa HlyE

YebF CmR vector. Expected size is ≈2800 bp. Lanes: (1) 2Log DNA page ruler, (2-5) PCR reaction products.

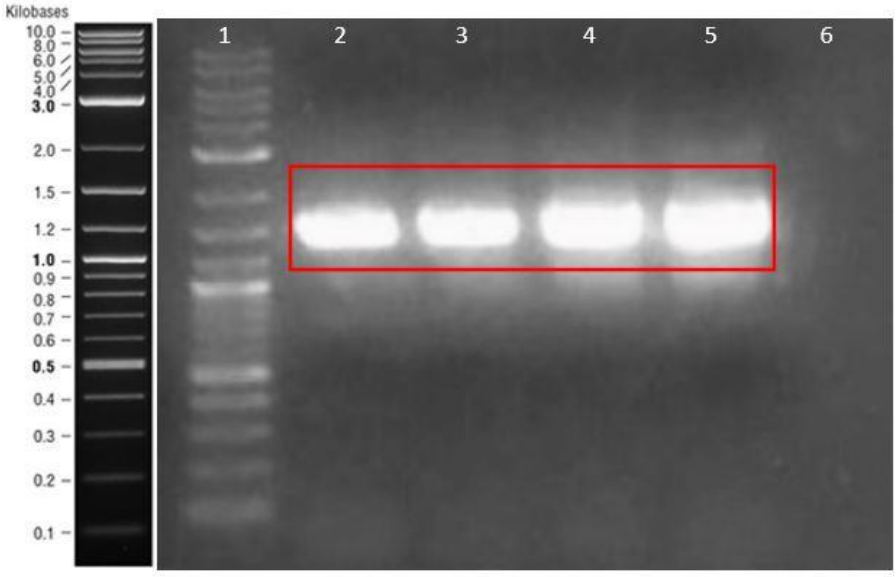

Figure 36. Gel Electrophoresis of PCR products performed for the amplification of the Hemolysin E. JO29 and EK pBAD rev were used as primers and the template was pZa pL-tetO YebF HlyE 6his CmR vector. Expected size is ≈1393 bp. Lanes: (1) 2Log DNA page ruler, (2-5) PCR reaction products (6) Negative Control.

After cloning the parts, Gibson Assembly was performed, and the end product of the reaction was chemically transformed into *E. coli* PRO DH5α. After transformation different colonies were selected and colony PCR was performed to check the validity of the cloning. To do colony PCR JO5 and EK pBAD rev primers were used and gel electrophoresis was run using the PCR reaction products.

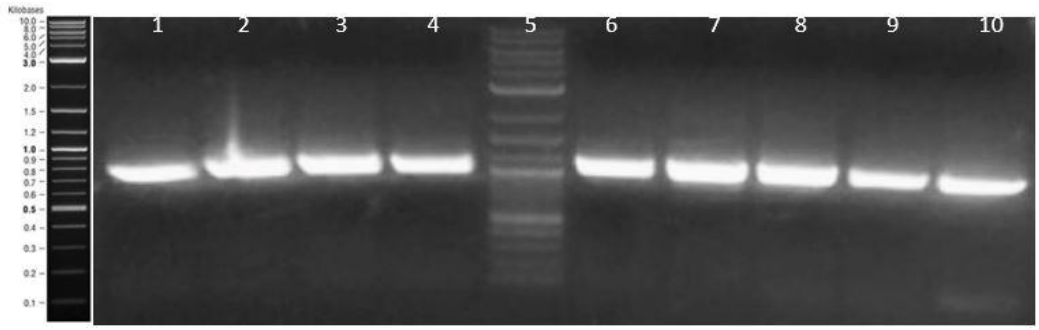

Figure 37. Gel Electrophoresis of colony PCR products. JO5 and EK pBAD rev were used as primers. Expected size is ≈1024 kb. Lanes: (1-4&6-10) PCR products of different colonies, (5) 2Log DNA ladder.

3.4.7 Verification of HlyE secretion using pZA native pTetO HlyE Yebf 6xHis CmR vector

After proving with colony PCR that the cloning was performed correctly two colonies were sent for sequencing. After verification via sequencing the correct plasmid was chemically transformed to *E. coli* BL21 (DE3). After transformation western blotting was performed to check the protein expression at different temperatures. Western Blotting was performed both in *E. coli* BL21 (DE3) and *E. coli* PRO DH5α.

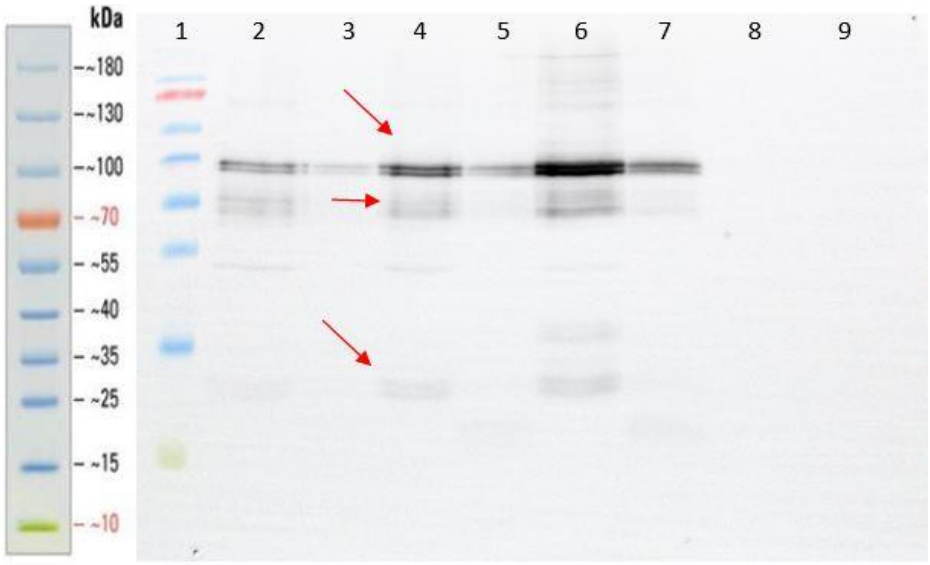

Figure 38. Western Blotting to control hemolysin E expression under different induction conditions. Lanes: (1) Page Ruler Protein Ladder, (2) *E. coli* BL21 (DE3)* whole cell (induced at 37°C), (3) *E. coli* BL21 (DE3)* supernatant (induced at 37°C), (4) *E. coli* BL21 (DE3)* whole cell (induced at 30°C), (5) *E. coli* BL21 (DE3)* supernatant (induced at 30°C), (6) *E. coli* BL21 (DE3)* whole cell (induced at 18°C), (7) *E. coli* BL21 (DE3)* supernatant (induced at 18°C), (8) *E. coli* BL21 (DE3) whole cell (induced at 37°C), (9) *E. coli* BL21 (DE3) supernatant (induced at 37°C). ('*' corresponds to pZA native pTetO HlyE Yebf 6xHis CmR).

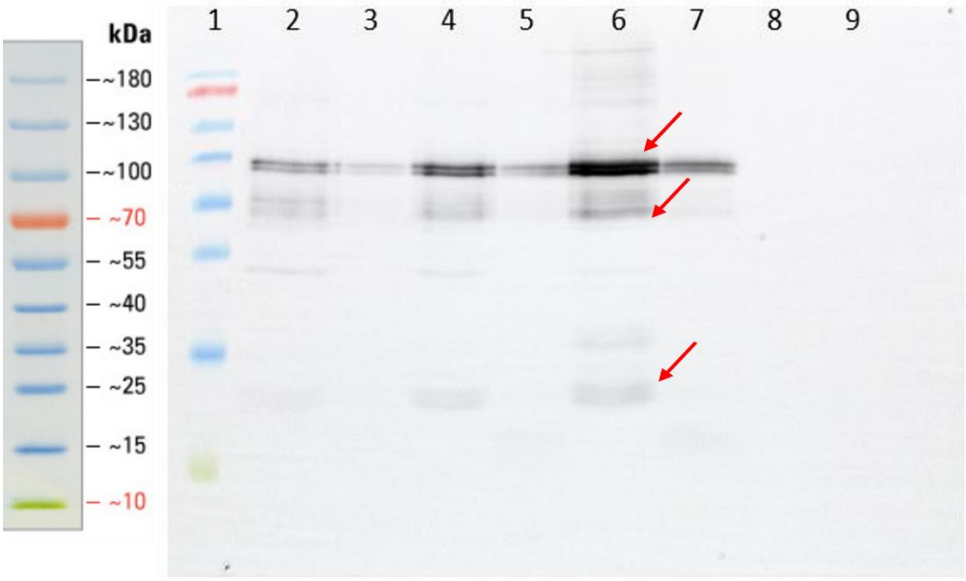

Figure 39. Western Blotting to control hemolysin E expression in *E. coli* PRO DH5α under different induction conditions. Lanes: (1) Page Ruler Protein Ladder, (2) *E. coli* PRO DH5α * whole cell (induced at 37°C), (3) *E. coli* PRO DH5α * supernatant (induced at 37°C), (4) *E. coli* PRO DH5α * whole cell (induced at 30°C), (5) *E. coli* PRO DH5α * supernatant (induced at 30°C), (6) *E. coli* PRO DH5α * whole cell (induced at 18°C), (7) *E. coli* PRO DH5α * supernatant (induced at 18°C), (8) *E. coli* PRO DH5α whole cell (induced at 37°C), (9) *E. coli* PRO DH5α supernatant (induced at 37°C). ('*' corresponds to pZA native pTetO HlyE Yebf 6xHis CmR).

All supernatant samples were concentrated via TCA protein precipitation method. Via western blotting we were able to prove that our protein was being secreted to the outer surface of *E. coli* and our secretion system was properly working. As seen for both pictures there seem to be three visible bands which are also marked by the red arrows. Regarding the top band it appears to have a size of ≈46 kDA which corresponds with the size of the fusion hemolysin E and YebF tag. The second band is around 33 kDa which

means that some fusion protein HlyE YebF is separated during sample preparation, and it corresponds to HlyE. Regarding the lowest band it corresponds to the YebF (≈13 kDa).

3.5 Testing the bacteria in breast cancer cells

3.5.1 Testing the bacteria in cell culture.

After constructing our binding and secretion system we tried our constructs into mammalian cells to see their efficacy. For these experiments Jimt1 mammalian breast cancer cells were grown in T25 cm^2 flask and when the confluency reached 80-90% the cells were counted and 10^4 mammalian cells were plated in each well in a 96 well plate.

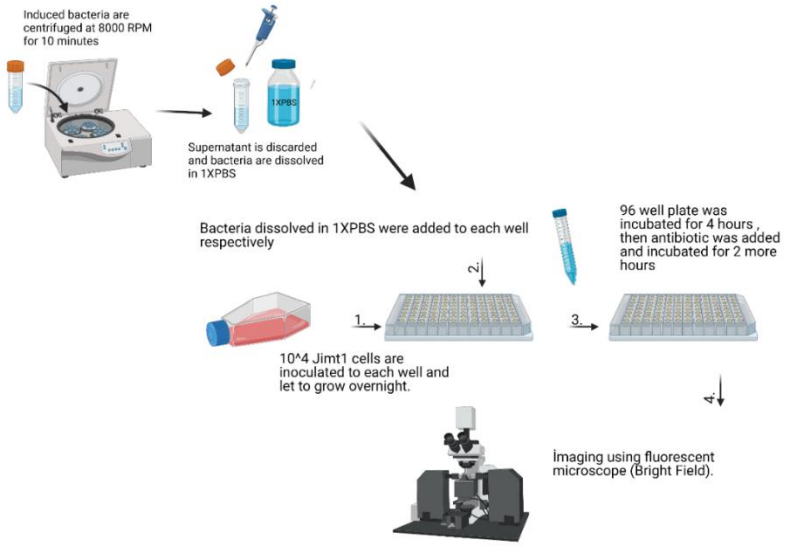

Figure 40. Schematic representation of bacteria efficacy evaluation.

Afterwards the cells were let grow for 1 day till they reach a confluency of ≈80%. During the waiting period i. *E. coli* BL21 (DE3); ii. *E. coli* BL21 (DE3) pZA native pTetO HlyE Yebf 6xHis CmR and iii. *E. coli* BL21 (DE3) pET22b T7-LacO pelb 2Rs15d Ag43 AmpR, pZA native pTetO HlyE Yebf 6xHis CmR cells were induced with aTc and/or 1 mM IPTG respectively for 24 hours at 30°C. After induction, OD_{600} was measured for every sample in order to calculate the number of bacteria. An OD_{600} of 1 roughly corresponds with 10^8 bacteria (*E. coli*) per mL. The cells were centrifuged at 8000 RPM for 10 minutes and the supernatant was discarded. The pellet was dissolved in 1X PBS. Later on, 5*10^5 bacteria were added to each well consisting of 10^4 mammalian cells. Before addition of the bacteria the original media of the mammalian cells was removed, the mammalian cells were washed with 1X PBS and 100 μL of Jimt1 growth media lacking FBS (fetal bovine serum) and antibiotic was added. The bacteria and mammalian cells were incubated together at 37°C overnight and microscope pictures were taken under the fluorescent microscope.

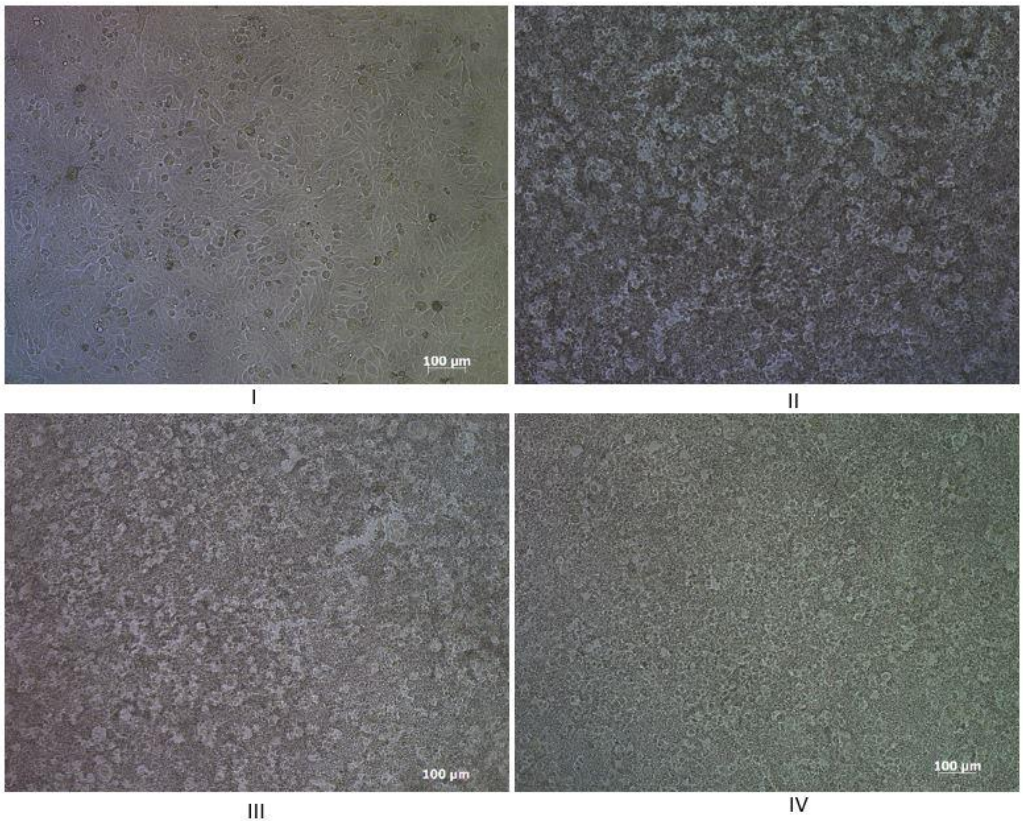

Figure 41. Fluoresence Microscopy (Bright Field) pictures. Scale bar 100 µm for all pictures. (I) Jimt1 mammalian cells grown in fully suplemented DMEM, (II) Jimt1 mammalian cells and *E. coli* BL21 (DE3) cocultured, (III) Jimt1 mammalian cells and *E. coli* BL21 (DE3) pZA native pTetO HlyE Yebf 6xHis CmR cocultured, (IV) Jimt1 mammalian cells and *E. coli* BL21 (DE3) pET22b T7-LacO pelb 2Rs15d Ag43 AmpR, pZA native pTetO HlyE Yebf 6xHis CmR cocultured.

According to the bright field microscope pictures we couldn't conclude if our bacteria were killing the mammalian breast cancer cells. Moreover we couldn't perform MTT assay under these conditions because the residual bacteria would affect the MTT results.

3.5.2 Testing the supernatant in cell culture

Under these circumstances we decided to test the efficacy of our bacteria by coculturing the mammalian cells with the supernatant of our bacteria, since we had already proven the expression of our toxin in the extracellular surface. In this case *E. coli* BL21 (DE3) pZA native pTetO HlyE Yebf 6xHis CmR cells and *E. coli* PRO DH5α pZA native pTetO HlyE Yebf 6xHis CmR were induced with aTc at 30°C for 24 hours. Upon induction supernatant was separated by centrifugation at 8000 RPM (rotation per minute) for 10 minutes. Later on, the supernatant (20 mL) was concentrated to a final volume of 5 mL using a 10 kDA protein concentration falcon and filtered with 0,22 μm sterile filters. The collected product was administrated to the 96 well plates consisting of the Jimt1 mammalian cells. The mammalian cells were incubated together with the supernatant for 48 hours and after the incubation period, MTT assay was performed, OD_{570} was measured, and statistical analysis were made.

Sample Name	**OD_{570} Measurement for Replicas (1-3)**		
DMEM	1,5823	1,6801	1,7519
Pro Empty 200μL	1,0738	1,3842	1,3289
Pro HlyE 200 μL	0,9065	1,0286	0,863
BL21 empty 200 μL	0,9838	1,0646	1,1784
BL21 HlyE 200 μL	0,6178	0,5573	0,6988

Table 2. OD_{570nm} measurements for supernatant toxicity assay experiment.

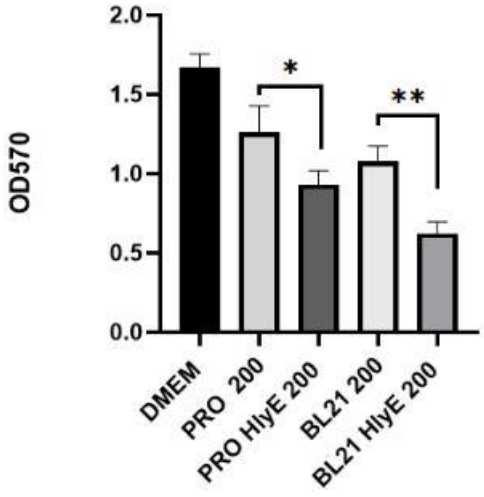

Figure 42. Unpaired t test statistical analysis was performed to compare cell viability in different conditions. Based on unpaired t test significant difference, with a value of $p \leq 0.05$, $p \leq 0.01$, $p \leq 0.001$ are shown with "*", "**", "***" respectively.

According to this data we conclude that the supernatant of the cells secreting the toxin was killing Jimt1 mammalian breast cancer cells.

3.6 Testing the bacteria in jimt1 spheroids

3.6.1 Jimt1 spheroid formation

In order to test our bacteria in 3D cell culture environment we decided to create spheroids. Spheroids are 3D cellular platforms that can be used for drug testing. The spheroids aim to preserve the tumor characteristics more than the traditional monolayer cell culturing (50). To build the spheroids first a Jimt1 cell stock was opened, and cells were plated into a T25 cm^2 flask. When the confluency reached a level of 80-90% the cells were detached from the flask and counted as explained in the materials and methods section. Meanwhile high purity agarose gel was prepared and autoclaved.

Afterwards 40 µL of gel (melting at 150 °C was applied when necessary) was placed into each well of a 96 well plate and let solidify for about 15-20 minutes. After the solidification the Jimt1 cells dissolved in 100 µL Jimt1 were added to each well at different concentrations. In different wells 1000, 1500, 2000, 2500, 3000 cells were added and the 96 well plate was incubated into the incubator for 4 days. On the third day 50 µL of media was carefully extracted from each well and 100 µL of fresh growth media was added.

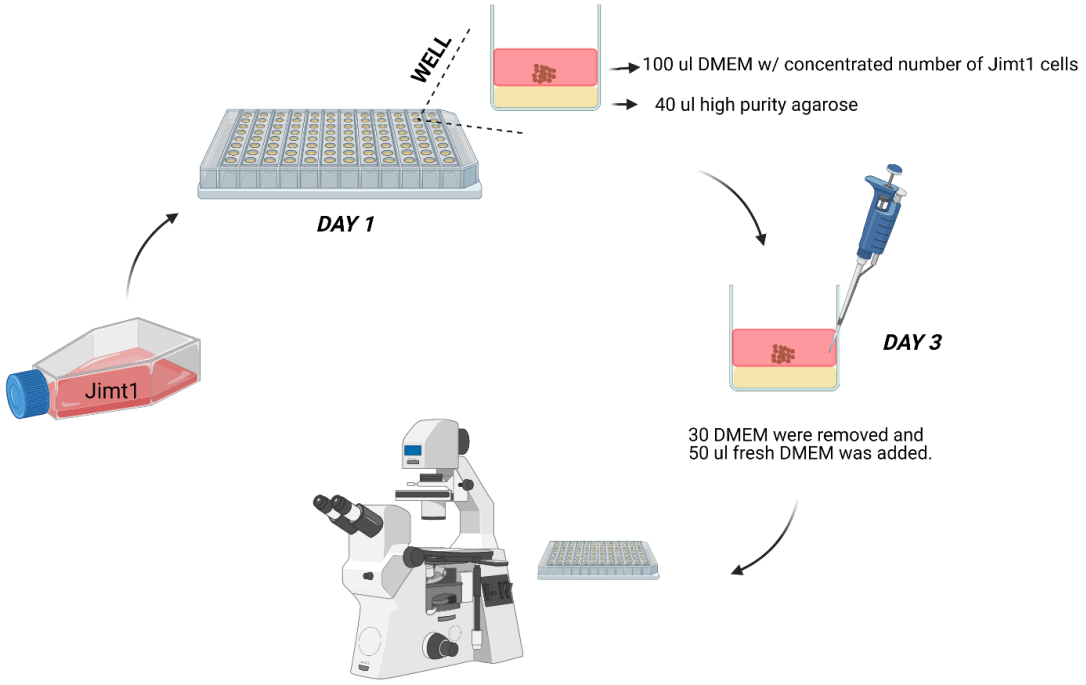

Figure 43. Schematic representation of spheroid preparation workflow. During the first day 40 µL of high purity agarose gel was added to each well and Jimt1 mammalian breast cancer cells dissolved in 1mL growth media were added on top of the gel. On the third day 50 µL of media was carefully removed and 100 µL fresh media was added. One day later the spheroids were ready for use.

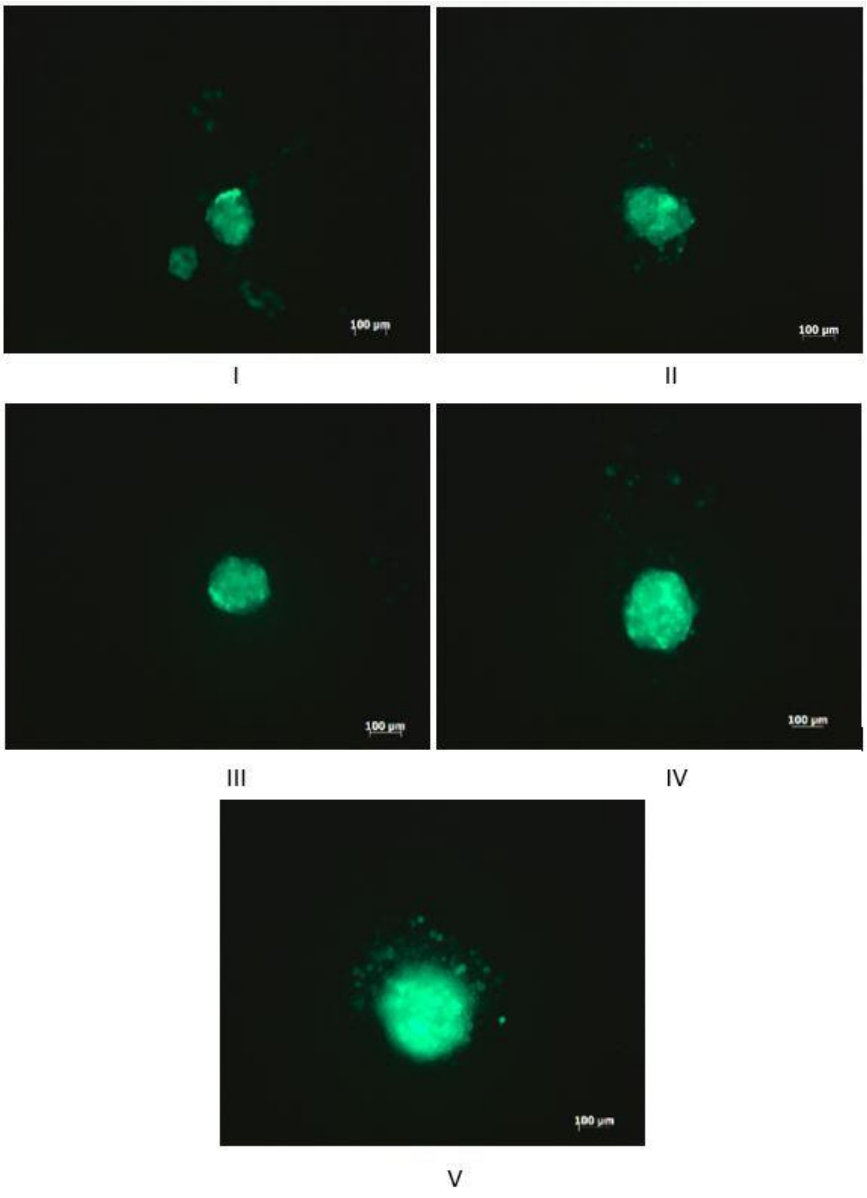

Figure 44. Fluorescence Microscopy pictures of Jimt1 breast cancer cells spheroids. Jimt1 breast cancer cells appearing in green as they have been stably transfected with GFP. (I) Spheroid consisting of 1000 Jimt1 cells, (II) Spheroid created using 1500 Jimt1

cells, (III) Spheroid created using 2000 Jimt1 cells, (IV) Spheroid created using 2500 Jimt1 cells, (V) Spheroid created using 3000 Jimt1 cells.

At the end of the fourth day fluorescence microscopy pictures were taken and the best cell concentration for spheroid formation using Jimt1 cells was determined. The diameter of the spheroids should be around 300 μm to avoid necrosis which would cause the death of the cells at the center therefore in our case we decided to continue with 2500 cells per well which created the spheroids with the closest diameter to our goal.

3.6.2 Testing bacteria efficacy on Jimt1 spheroid

After constructing the spheroids, we decided to test the supernatant from our bacteria and check bacterial efficacy. To perform the experiment a similar strategy with testing our bacteria in 2D was followed. First spheroids were prepared in full mammalian cell growth media lacking antibiotic and FBS. During the waiting period bacteria containing only the toxin construct or both the toxin and nanobody constructs were induced. Later on, 10^4 bacteria dissolved in 1xPBS were inoculated to each well consisting of the spheroids. The bacteria and spheroids were incubated together at 37°C incubator for four hours and after that antibiotic was added to each well to kill the bacteria. The other day fluorescent microscope pictures were taken.

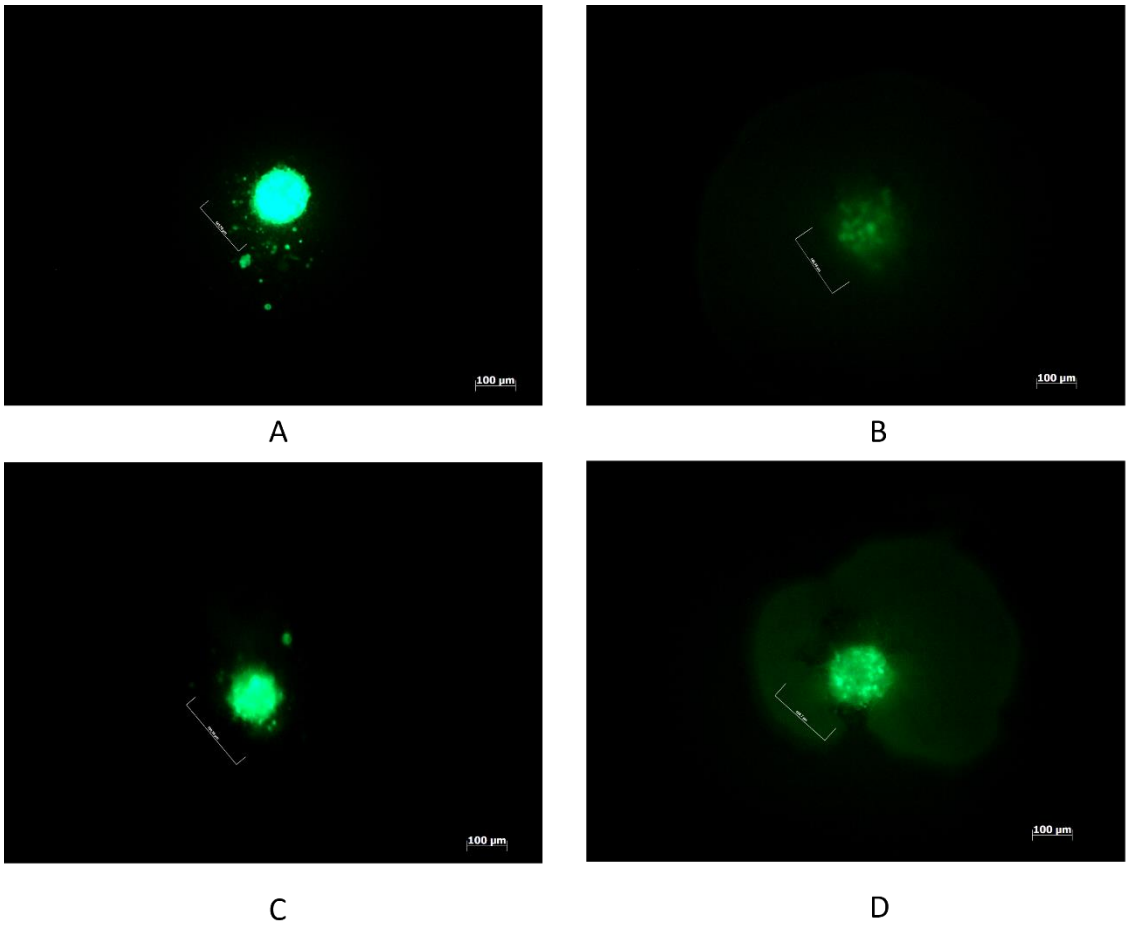

Figure 45. Fluorescent microscope pictures of Jimt1 spheroids treated with bacteria. (A) Spheroids grown in full DMEM. (B) Spheroids treated with BL21 (DE3). (C) Spheroids treated with BL21 (DE3) pZA native pTetO HlyE Yebf 6xHis CmR. (D) Spheroid treated with BL21 (DE3) pZA native pTetO HlyE Yebf 6xHis CmR pET22b T7-LacO pelb 2Rs15d Ag43 AmpR bacteria. (Jimt1 cells in green). Bacteria were inoculated for 4 hours at 37°C and after that antibiotic was added to kill the bacteria. The other day microscope pictures were taken.

From the pictures that were taken under fluorescence microscope we understand that all tested bacteria have some effect on Jimt1 breast cancer cell viability. Regarding the BL21 (DE3) pZA native pTetO HlyE Yebf 6xHis CmR, pET22b T7-LacO pelb 2Rs15d

Ag43 AmpR cells, there seems to be a volume of dead Jimt1 cells spread at the vicinity of the spheroid appearing as green. Using this preliminary data, *E. coli* that was transformed with both nanobody and toxin seems to be more promising in killing Jimt1, compared to empty BL21 (DE3) and BL21 (DE3) transformed only with toxin construct. Anyhow further experimentation is required for a better understanding.

CHAPTER 4

CONCLUSION

In this study, a cellular device that can express a nanobody on its surface and bind to Jimt1 breast cancer cell was developed. Ag43 autotransporter protein was used for the expression of 2Rs15d nanobody at the surface of *E. coli* and a binding assay was designed to control the binding affinity of the nanobody. Alongside that, Hemolysin E (HlyE), a pore forming toxin was produced both intracellularly and extracellularly in *E. coli* BL21 (DE3). For secretion of Hemolysin E to the extracellular space three different strategies; one involving Ag43, and two involving YebF secretion systems, were tested and YebF resulted to be the most successful one. Purified Hemolysin E, as well as the supernatant from *E. coli* BL21 (DE3) pZA native pTetO HlyE Yebf 6xHis CmR cells were shown to kill Jimt1 breast cancer cells *in vitro*. Jimt1 spheroids, which are 3D platforms used for therapeutic testing, were built and the engineered bacterial constructs were tested. From the preliminary data with fluorescence pictures, we can hypothesize that *E. coli* BL21 (DE3) expressing both the nanobody and the toxin shows more toxic activity towards Jimt1 spheroids compared to *E. coli* BL21 (DE3) and *E. coli* BL21 (DE3) expressing the toxin. This construct is promising but further experimentation is required for a proper understanding and evaluation.

Overall, with this approach, two of the major challenges of the current tumor treatment methodologies were aimed to overcome. The first one being specific targeting on the tumor site and the second one; efficient delivery of therapeutic agent. The secretion and binding platforms developed in this study can be implemented in nonpathogenic,

probiotic bacteria for further evaluation *in vivo.* In order to transform the platform for *in vivo* testing different conditions such as selection of the bacteria, immune system clearance, antibiotic resistance, and number of bacteria to be administered should be taken into consideration. To have a controlled release system for the therapeutic agent a quorum sensing mechanism can be integrated into the engineered bacteria. Quorum sensing is a regulatory system at transcription level in bacteria based on cell density. By using this system bacteria can eliminate themselves once they reach a population density that would be dangerous for the human body. Using the various tools offered by synthetic biology these platforms can be further modified to meet the necessities for *in vivo* application.

BIBLIOGRAPHY

[1] Benner, S. A., & Sismour, A. M. (2005). Synthetic biology. Nature reviews. Genetics, 6(7), 533–543. https://doi.org/10.1038/nrg1637

[2] Hoffman RM. (ed.) Bacterial Therapy of Cancer: Methods and Protocols. Methods in Molecular Biology. Volume 1409. Totowa: Humana Press Inc; 2016. p. 1–186

[3] McCarthy E. F. (2006). The toxins of William B. Coley and the treatment of bone and soft-tissue sarcomas. The Iowa orthopaedic journal, 26, 154–158.

[4] Richardson, M. A., Ramirez, T., Russell, N. C., & Moye, L. A. (1999). Coley toxins immunotherapy: a retrospective review. Alternative therapies in health and medicine, 5(3), 42–47.

[5] Pflock, M., Kennard, S., Delany, I., Scarlato, V., & Beier, D. (2005). Acid-induced activation of the urease promoters is mediated directly by the ArsRS two-component system of Helicobacter pylori. Infection and immunity, 73(10), 6437–6445. https://doi.org/10.1128/IAI.73.10.6437-6445.2005

[6] Rodrigues, J. L., & Rodrigues, L. R. (2018). Potential Applications of the Escherichia coli Heat Shock Response in Synthetic Biology. Trends in biotechnology, 36(2), 186–198. https://doi.org/10.1016/j.tibtech.2017.10.014

[7] Zhang, B., Georgiev, O., Hagmann, M., Günes, C., Cramer, M., Faller, P., Vasák, M., & Schaffner, W. (2003). Activity of metal-responsive transcription factor 1 by toxic heavy metals and H2O2 in vitro is modulated by metallothionein. Molecular and cellular biology, 23(23), 8471–8485. https://doi.org/10.1128/MCB.23.23.8471-8485.2003

[8] Ono, A., Ito, A., Sato, T., Yamaguchi, M., Suzuki, T., Kawabe, Y., & Kamihira, M. (2017). Hypoxia-responsive transgene expression system using RTP801 promoter and synthetic transactivator fused with oxygen-dependent degradation domain. Journal of bioscience and bioengineering, 124(1), 115–124. https://doi.org/10.1016/j.jbiosc.2017.02.012

[9] Chou, C. H., Aristidou, A. A., Meng, S. Y., Bennett, G. N., & San, K. Y. (1995). Characterization of a pH-inducible promoter system for high-level expression of recombinant proteins in Escherichia coli. Biotechnology and bioengineering, 47(2), 186–192. https://doi.org/10.1002/bit.260470210

[10] Cancer. (2019, July 12). WHO | World Health Organization. https://www.who.int/health-topics/cancer#tab=tab_1

[11] Arruebo, M., Vilaboa, N., Sáez-Gutierrez, B., Lambea, J., Tres, A., Valladares, M., & González-Fernández, A. (2011). Assessment of the evolution of cancer treatment therapies. Cancers, 3(3), 3279–3330. https://doi.org/10.3390/cancers3033279

[12] Zhang, B., Li, A., Zuo, F., Yu, R., Zeng, Z., Ma, H., & Chen, S. (2016). Recombinant Lactococcus lactis NZ9000 secretes a bioactive kisspeptin that inhibits

proliferation and migration of human colon carcinoma HT-29 cells. Microbial cell factories, 15(1), 102. https://doi.org/10.1186/s12934-016-0506-7

[13] Mi, Z., Feng, Z. C., Li, C., Yang, X., Ma, M. T., & Rong, P. F. (2019). Salmonella-Mediated Cancer Therapy: An Innovative Therapeutic Strategy. Journal of Cancer, 10(20), 4765–4776. https://doi.org/10.7150/jca.32650

[14] Lee C. H. (2012). Engineering bacteria toward tumor targeting for cancer treatment: current state and perspectives. Applied microbiology and biotechnology, 93(2), 517–523. https://doi.org/10.1007/s00253-011-3695-3

[15] Chang, W. W., & Lee, C. H. (2014). Salmonella as an innovative therapeutic antitumor agent. International journal of molecular sciences, 15(8), 14546–14554. https://doi.org/10.3390/ijms150814546

[16] Schulte, M., & Hensel, M. (2016). Models of intestinal infection by Salmonella enterica: introduction of a new neonate mouse model. F1000Research, 5, F1000 Faculty Rev-1498. https://doi.org/10.12688/f1000research.8468.1

[17] Forbes, N. S., Coffin, R. S., Deng, L., Evgin, L., Fiering, S., Giacalone, M., Gravekamp, C., Gulley, J. L., Gunn, H., Hoffman, R. M., Kaur, B., Liu, K., Lyerly, H. K., Marciscano, A. E., Moradian, E., Ruppel, S., Saltzman, D. A., Tattersall, P. J., Thorne, S., Vile, R. G., … McFadden, G. (2018). White paper on microbial anti-cancer therapy and prevention. Journal for immunotherapy of cancer, 6(1), 78. https://doi.org/10.1186/s40425-018-0381-3

[18] Uchugonova, A., Zhang, Y., Salz, R., Liu, F., Suetsugu, A., Zhang, L., Koenig, K., Hoffman, R. M., & Zhao, M. (2015). Imaging the Different Mechanisms of Prostate Cancer Cell-killing by Tumor-targeting Salmonella typhimurium A1-R. Anticancer research, 35(10), 5225–5229.

[19] Yu, B., Yang, M., Shi, L., Yao, Y., Jiang, Q., Li, X., Tang, L. H., Zheng, B. J., Yuen, K. Y., Smith, D. K., Song, E., & Huang, J. D. (2012). Explicit hypoxia targeting with tumor suppression by creating an "obligate" anaerobic Salmonella Typhimurium strain. Scientific reports, 2, 436. https://doi.org/10.1038/srep00436

[20] Ryan, R. M., Green, J., Williams, P. J., Tazzyman, S., Hunt, S., Harmey, J. H., Kehoe, S. C., & Lewis, C. E. (2009). Bacterial delivery of a novel cytolysin to hypoxic areas of solid tumors. Gene therapy, 16(3), 329–339. https://doi.org/10.1038/gt.2008.188

[21] Crack, J. C., Le Brun, N. E., Thomson, A. J., Green, J., & Jervis, A. J. (2008). Reactions of nitric oxide and oxygen with the regulator of fumarate and nitrate reduction, a global transcriptional regulator, during anaerobic growth of Escherichia coli. Methods in enzymology, 437, 191–209. https://doi.org/10.1016/S0076-6879(07)37011-0

[22] Vaupel, P., Kallinowski, F., & Okunieff, P. (1989). Blood flow, oxygen and nutrient supply, and metabolic microenvironment of human tumors: a review. Cancer research, 49(23), 6449–6465.

[23] Boedtkjer, E., Moreira, J. M., Mele, M., Vahl, P., Wielenga, V. T., Christiansen, P. M., Jensen, V. E., Pedersen, S. F., & Aalkjaer, C. (2013). Contribution of Na+,HCO3(-)-cotransport to cellular pH control in human breast cancer: a role for the breast cancer susceptibility locus NBCn1 (SLC4A7). International journal of cancer, 132(6), 1288–1299. https://doi.org/10.1002/ijc.27782

[24] Chien, T., Harimoto, T., Kepecs, B., Gray, K., Coker, C., Hou, N., Pu, K., Azad, T., Nolasco, A., Pavlicova, M., & Danino, T. (2021). Enhancing the tropism of bacteria via genetically programmed biosensors. Nature biomedical engineering, 10.1038/s41551-021-00772-3. Advance online publication. https://doi.org/10.1038/s41551-021-00772-3

[25] Haziza, C., Stragier, P., & Patte, J. C. (1982). Nucleotide sequence of the asd gene of Escherichia coli: absence of a typical attenuation signal. The EMBO journal, 1(3), 379–384.

[26] Panteli, J. T., & Forbes, N. S. (2016). Engineered bacteria detect spatial profiles in glucose concentration within solid tumor cell masses. Biotechnology and bioengineering, 113(11), 2474–2484. https://doi.org/10.1002/bit.26006

[27] Xu-Monette, Z. Y., Zhang, M., Li, J., & Young, K. H. (2017). PD-1/PD-L1 Blockade: Have We Found the Key to Unleash the Antitumor Immune Response?. Frontiers in immunology, 8, 1597. https://doi.org/10.3389/fimmu.2017.01597

[28] Kalantari Khandani, N., Ghahremanloo, A., & Hashemy, S. I. (2020). Role of tumor microenvironment in the regulation of PD-L1: A novel role in resistance to cancer immunotherapy. Journal of cellular physiology, 235(10), 6496–6506. https://doi.org/10.1002/jcp.29671

[29] Gurbatri, C. R., Lia, I., Vincent, R., Coker, C., Castro, S., Treuting, P. M., Hinchliffe, T. E., Arpaia, N., & Danino, T. (2020). Engineered probiotics for local tumor delivery of checkpoint blockade nanobodies. Science translational medicine, 12(530), eaax0876. https://doi.org/10.1126/scitranslmed.aax0876

[30] Liu, Z., Wang, F., & Chen, X. (2008). Integrin alpha(v)beta(3)-Targeted Cancer Therapy. Drug development research, 69(6), 329–339. https://doi.org/10.1002/ddr.20265

[31] Park, S. H., Zheng, J. H., Nguyen, V. H., Jiang, S. N., Kim, D. Y., Szardenings, M., Min, J. H., Hong, Y., Choy, H. E., & Min, J. J. (2016). RGD Peptide Cell-Surface Display Enhances the Targeting and Therapeutic Efficacy of Attenuated Salmonella-mediated Cancer Therapy. Theranostics, 6(10), 1672–1682. https://doi.org/10.7150/thno.16135

[32] Bereta, M., Hayhurst, A., Gajda, M., Chorobik, P., Targosz, M., Marcinkiewicz, J., & Kaufman, H. L. (2007). Improving tumor targeting and therapeutic potential of Salmonella VNP20009 by displaying cell surface CEA-specific antibodies. Vaccine, 25(21), 4183–4192. https://doi.org/10.1016/j.vaccine.2007.03.008

[33] Piñero-Lambea, C., Bodelón, G., Fernández-Periáñez, R., Cuesta, A. M., Álvarez-Vallina, L., & Fernández, L. Á. (2015). Programming controlled adhesion of E. coli to

target surfaces, cells, and tumors with synthetic adhesins. ACS synthetic biology, 4(4), 463–473. https://doi.org/10.1021/sb500252a

[34] Flentie, K. et al. A bioluminescent transposon reporter-trap identifies tumor-specific microenvironment-induced promoters in Salmonella for conditional bacterial-based tumor therapy. Cancer Discov. 2, 624–637 (2012)

[35] Yu, B., Yang, M., Shi, L. et al. Explicit hypoxia targeting with tumor suppression by creating an "obligate" anaerobic Salmonella Typhimurium strain. Sci Rep 2, 436 (2012). https://doi.org/10.1038/srep00436

[36] Dai, Y. M., Toley, B. J., Swofford, C. A. & Forbes, N. S. Construction of an inducible cell-communication system that amplifies Salmonella gene expression in tumor tissue. Biotechnol. Bioeng. 110, 1769–1781 (2013)

[37] Kim, K. et al. Cell mass-dependent expression of an anticancer protein drug by tumor-targeted Salmonella. Oncotarget 9, 8548–8559 (2018)

[38] Jiang, S. N. et al. Inhibition of tumor growth and metastasis by a combination of Escherichia coli-mediated cytolytic therapy and radiotherapy. Mol. Ther. 18, 635–642 (2010).

[39] Jiang, S. N. et al. Engineering of bacteria for the visualization of targeted delivery of a cytolytic anticancer agent. Mol. Ther. 21, 1985–1995 (2013).

[40] Duong, M. T. Q., Qin, Y., You, S. H., & Min, J. J. (2019). Bacteria-cancer interactions: bacteria-based cancer therapy. Experimental & molecular medicine, 51(12), 1-15.

[41] Riss TL, Moravec RA, Niles AL, et al. Cell Viability Assays. 2013 May 1 [Updated 2016 Jul 1]. In: Markossian S, Grossman A, Brimacombe K, et al., editors. Assay Guidance Manual [Internet]. Bethesda (MD): Eli Lilly & Company and the National Center for Advancing Translational Sciences; 2004-. Available from: https://www.ncbi.nlm.nih.gov/books/NBK144065/

[42] Vaneycken, I., Devoogdt, N., Van Gassen, N., Vincke, C., Xavier, C., Wernery, U., Muyldermans, S., Lahoutte, T., & Caveliers, V. (2011). Preclinical screening of anti-HER2 nanobodies for molecular imaging of breast cancer. FASEB journal : official publication of the Federation of American Societies for Experimental Biology, 25(7), 2433–2446. https://doi.org/10.1096/fj.10-180331

[43] Bannas, P., Hambach, J., & Koch-Nolte, F. (2017). Nanobodies and Nanobody-Based Human Heavy Chain Antibodies As Antitumor Therapeutics. Frontiers in immunology, 8, 1603. https://doi.org/10.3389/fimmu.2017.01603

[44] Ahan, R. E., Kırpat, B. M., Saltepe, B., & Şeker, U. (2019). A Self-Actuated Cellular Protein Delivery Machine. ACS synthetic biology, 8(4), 686–696. https://doi.org/10.1021/acssynbio.9b00062

[45] Ling, Z., Dayong, C., Denggao, Y., Yiting, W., Liaoqiong, F., & Zhibiao, W. (2019). Escherichia Coli Outer Membrane Vesicles Induced DNA Double-Strand

Breaks in Intestinal Epithelial Caco-2 Cells. Medical science monitor basic research, 25, 45–52. https://doi.org/10.12659/MSMBR.913756

[46] Jayaraman, P., Holowko, M. B., Yeoh, J. W., Lim, S., & Poh, C. L. (2017). Repurposing a Two-Component System-Based Biosensor for the Killing of Vibrio cholerae. ACS synthetic biology, 6(7), 1403–1415. https://doi.org/10.1021/acssynbio.7b00058

[47] Zhou, Z., Li, Q., Xu, R., Wang, B., Du, G., & Kang, Z. (2019). Secretory expression of the rat aryl sulfotransferases IV with improved catalytic efficiency by molecular engineering. 3 Biotech, 9(6), 246. https://doi.org/10.1007/s13205-019-1781-x

[48] Chen, N., Hong, F. L., Wang, H. H., Yuan, Q. H., Ma, W. Y., Gao, X. N., Shi, R., Zhang, R. J., Sun, C. S., & Wang, S. B. (2012). Modified recombinant proteins can be exported via the Sec pathway in Escherichia coli. PloS one, 7(8), e42519. https://doi.org/10.1371/journal.pone.0042519

[49] Prehna, G., Zhang, G., Gong, X., Duszyk, M., Okon, M., McIntosh, L. P., Weiner, J. H., & Strynadka, N. C. (2012). A protein export pathway involving Escherichia coli porins. Structure (London, England : 1993), 20(7), 1154–1166. https://doi.org/10.1016/j.str.2012.04.014

[50] Ishiguro, T., Ohata, H., Sato, A., Yamawaki, K., Enomoto, T., & Okamoto, K. (2017). Tumor-derived spheroids: Relevance to cancer stem cells and clinical applications. Cancer science, 108(3), 283–289. https://doi.org/10.1111/cas.13155

APPENDIX A

DNA sequences of main genetic elements used in this study

GENE NAME	*DNA SEQUENCE (5'-3')*
2Rs15D gene	CAGGTGCAGCTGCAGGAAAGCGGCGGCGGCAGCGTGCAG GCGGGCGGCAGCCTGAAACTGACCTGCGCGGCGAGCGGC TATATTTTTAACAGCTGCGGCATGGGCTGGTATCGCCAGA GCCCGGGCCGCGAACGCGAACTGGTGAGCCGCATTAGCG GCGATGGCGATACCTGGCATAAAGAAAGCGTGAAAGGCC GCTTTACCATTAGCCAGGATAACGTGAAAAAAACCCTGTA TCTGCAGATGAACAGCCTGAAACCGGAAGATACCGCGGT GTATTTTTGCGCGGTGTGCTATAACCTGGAAACCTATTGG GGCCAGGGCACCCAGGTGACCGTGAGCAGC
2Rs15D ordered fragement	GCCCAGCCGGCGATGGCCATGGGCACTAGTCAGGTGCAG CTGCAGGAAAGCGGCGGCGGCAGCGTGCAGGCGGGCGGC AGCCTGAAACTGACCTGCGCGGCGAGCGGCTATATTTTTA ACAGCTGCGGCATGGGCTGGTATCGCCAGAGCCCGGGCC GCGAACGCGAACTGGTGAGCCGCATTAGCGGCGATGGCG ATACCTGGCATAAAGAAAGCGTGAAAGGCCGCTTTACCA TTAGCCAGGATAACGTGAAAAAAACCCTGTATCTGCAGA TGAACAGCCTGAAACCGGAAGATACCGCGGTGTATTTTTG CGCGGTGTGCTATAACCTGGAAACCTATTGGGGCCAGGG CACCCAGGTGACCGTGAGCAGCCTTAAGCGCACAACCAT

	CAATAAAAACGGT
pelB signal sequence	ATGAAATACCTGCTGCCGACCGCTGCTGCTGGTCTGCTGC TCCTCGCTGCCCAGCCGGCGATGGCC
160 N alpha subunit (Ag43 autotransporter protein)	CGCACAACCATCAATAAAAACGGTCGCCAGATTGTGAGA GCTGAAGGAACGGCAAATACCACTGTGGTTTATGCCGGC GGCGACCAGACTGTACATGGTCACGCACTGGATACCACG CTGAATGGGGGATACCAGTATGTGCACAACGGCGGTACA GCGTCTGACACTGTTGTGAACAGTGACGGCTGGCAGATTG TCAAAAACGGGGGTGTGGCCGGGAATACCACCGTTAATC AGAAGGGCAGACTGCAGGTGGACGCCGGTGGTACAGCCA CGAATGTCACCCTGAAGCAGGGCGGCGCACTGGTTACCA GTACGGCTGCAACCGTTACCGGCATAAACCGCCTGGGAG CATTCTCTGTTGTGGAGGGTAAAGCTGATAATGTCGTACT GGAAAATGGCGGACGCCTGGATGTGCTGACCGGACACAC AGCCACTAATACCCGCGTGGATGATGGCGGAACGCTGGA TGTCCGCAACGGTGGCACCGCCACCACCGTATCCATGGGA AATGGCGGTGTACTGCTGGCCGATTCCGGTGCCGCTGTCA GTGGTACCCGGAGCGACGGAAAGGCATTCAGTATCGGAG GCGGTCAGGCGGATGCCCTGATGCTGGAAAAAGGCAGTT CATTCACGCTGAACGCCGGTGATACGGCCACGGATACCA CGGTAAATGGCGGACTGTTCACCGCCAGGGGCGGCACAC TGGCGGGCACCACCACGCTGAATAACGGCGCCATACTTA CCCTTTCCGGGAAGACGGTGAACAACGATACCCTGACCAT

	CCGTGAAGGCGATGCACTCCTGCAGGGAGGCTCTCTCACC GGTAACGGCAGCGTGGAAAAATCAGGAAGTGGCACACTC ACTGTCAGCAACACCACACTCACCCAGAAAGCCGTCAAC CTGAATGAAGGCACGCTGACGCTGAACGACAGTACCGTC ACCACGGATGTCATTGCTCAGCGCGGTACAGCCCTGAAGC TGACCGGCAGCACTGTGCTGAACGGTGCCATTGAC
Beta subunit (Ag43 autotransporter protein)	CCCACGAATGTCACTCTCGCCTCCGGTGCCACCTGGAATA TCCCCGATAACGCCACGGTGCAGTCGGTGGTGGATGACCT CAGCCATGCCGGACAGATTCATTTCACCTCCACCCGCACA GGGAAGTTCGTACCGGCAACCCTGAAAGTGAAAAACCTG AACGGACAGAATGGCACCATCAGCCTGCGTGTACGCCCG GATATGGCACAGAACAATGCTGACAGACTGGTCATTGAC GGCGGCAGGGCAACCGGAAAAACCATCCTGAACCTGGTG AACGCCGGCAACAGTGCGTCGGGGCTGGCGACCAGCGGT AAGGGTATTCAGGTGGTGGAAGCCATTAACGGTGCCACC ACGGAGGAAGGGGCCTTTGTCCAGGGGAACAGGCTGCAG GCCGGTGCCTTTAACTACTCCCTCAACCGGGACAGTGATG AGAGCTGGTATCTGCGCAGTGAAAATGCTTATCGTGCAGA AGTCCCCCTGTATGCCTCCATGCTGACACAGGCAATGGAC TATGACCGGATTGTGGCAGGCTCCCGCAGCCATCAGACCG GTGTAAATGGTGAAAACAACAGCGTCCGTCTCAGCATTCA GGGCGGTCATCTCGGTCACGATAACAATGGCGGTATTGCC CGTGGGGCCACGCCGGAAAGCAGCGGCAGCTATGGATTC

	GTCCGTCTGGAGGGTGACCTGATGAGAACAGAGGTTGCC GGTATGTCTGTGACCGCGGGGGTATATGGTGCTGCTGGCC ATTCTTCCGTTGATGTTAAGGATGATGACGGCTCCCGTGC CGGCACGGTCCGGGATGATGCCGGCAGCCTGGGCGGATA CCTGAATCTGGTACACACGTCCTCCGGCCTGTGGGCTGAC ATTGTGGCACAGGGAACCCGCCACAGCATGAAAGCGTCA TCGGACAATAACGACTTCCGCGCCCGGGGCTGGGGCTGG CTGGGCTCACTGGAAACCGGTCTGCCCTTCAGTATCACTG ACAACCTGATGCTGGAGCCACAACTGCAGTATACCTGGC AGGGACTTTCCCTGGATGACGGTAAGGACAACGCCGGTT ATGTGAAGTTCGGGCATGGCAGTGCACAACATGTGCGTG CCGGTTTCCGTCTGGGCAGCCACAACGATATGACCTTTGG CGAAGGCACCTCATCCCGTGCCCCCCTGCGTGACAGTGCA AAACACAGTGTGAGTGAATTACCGGTGAACTGGTGGGTA CAGCCTTCTGTTATCCGCACCTTCAGCTCCCGGGGAGATA TGCGTGTGGGGACTTCCACTGCAGGCAGCGGGATGACGTT CTCTCCCTCACAGAATGGCACATCACTGGACCTGCAGGCC GGACTGGAAGCCCGTGTCCGGGAAAATATCACCCTGGGC GTTCAGGCCGGTTATGCCCACAGCGTCAGCGGCAGCAGC GCTGAAGGGTATAACGGTCAGGCCACACTGAATGTGACC TTC
HlyE gene	ATGACTGAAATCGTTGCAGATAAAACGGTAGAAGTAGTT AAAAACGCAATCGAAACCGCAGATGGAGCATTAGATCTT

	TATAATAAATATCTCGATCAGGTCATCCCCTGGCAGACCT TTGATGAAACCATAAAAGAGTTAAGTCGCTTTAAACAGG AGTATTCACAGGCAGCCTCCGTTTTAGTCGGCGATATTAA AACCTTACTTATGGATAGCCAGGATAAGTATTTTGAAGCA ACCCAAACAGTGTATGAATGGTGTGGTGTTGCGACGCAAT TGCTCGCAGCGTATATTTTGCTATTTGATGAGTACAATGA GAAGAAAGCATCCGCCCAGAAAGACATTCTCATTAAGGT ACTGGATGACGGCATCACGAAGCTGAATGAAGCGCAAAA ATCCCTGCTGGTAAGCTCACAAAGTTTCAACAACGCTTCC GGGAAACTGCTGGCGTTAGATAGCCAGTTAACCAATGATT TTTCAGAAAAAAGCAGCTATTTCCAGTCACAGGTAGATAA AATCAGGAAGGAAGCATATGCCGGTGCCGCAGCCGGTGT CGTCGCCGGTCCATTTGGATTAATCATTTCCTATTCTATTG CTGCGGGCGTAGTTGAAGGAAAACTGATTCCAGAATTGA AGAACAAGTTAAAATCTGTGCAGAATTTCTTTACCACCCT GTCTAACACGGTTAAACAAGCGAATAAAGATATCGATGC CGCCAAATTGAAATTAACCACCGAAATAGCCGCCATCGG TGAGATAAAAACGGAAACTGAAACAACCAGATTCTACGT TGATTATGATGATTTAATGCTTTCTTTGCTAAAAGAAGCG GCCAAAAAAATGATTAACACCTGTAATGAGTATCAGAAA AGACACGGTAAAAAGACACTCTTTGAGGTACCTGAAGTC
YebF	ATGAAAAAAAGAGGGGCGTTTTTAGGGCTGTTGTTGGTTT CTGCCTGCGCATCAGTTTTCGCTGCCAATAATGAAACCAG

	CAAGTCGGTCACTTTCCCAAAGTGTGAAGATCTGGATGCT GCCGGAATTGCCGCGAGCGTAAAACGTGATTATCAACAA AATCGCGTGGCGCGTTGGGCAGATGATCAAAAAATTGTC GGTCAGGCCGATCCCGTGGCTTGGGTCAGTTTGCAGGACA TTCAGGGTAAAGATGATAAATGGTCAGTACCGCTAACCGT GCGTGGTAAAAGTGCCGATATTCATTACCAGGTCAGCGTG GACTGCAAAGCGGGAATGGCGGAATATCAGCGGCGT
Sec signal	ATGAAAAAAAGAGGGGCGTTTTTAGGGCTGTTGTTGGTTT CTGCCTGCGCATCAGTTTTCGCT
T7 promoter	TAATACGACTCACTATAGG
LacO	GGAATTGTGAGCGGATAACAATTCC
T7 terminator	CTAGCATAACCCCTTGGGGCCTCTAAACGGGTCTTGAGGG GTTTTTTG
Native pTeO	TCCCTATCAGTGATAGAGA
rrnB T1 Terminator	CAAATAAAACGAAAGGCTCAGTCGAAAGACTGGGCCTTT CGTTTTATCTGTTGTTTGTCGGTGAACGCTCTCCTGAGTAG GACAAAT
PL-TetO	TCCCTATCAGTGATAGAGATTGACATCCCTATCAGTGATA GAGATACTGAGCACATCAGCAGGACGCACTGACC
GST tag	ATGTCCCCTATACTAGGTTATTGGAAAATTAAGGGCCTTG TGCAACCCACTCGACTTCTTTTGGAATATCTTGAAGAAAA ATATGAAGAGCATTTGTATGAGCGCGATGAAGGTGATAA ATGGCGAAACAAAAAGTTTGAATTGGGTTTGGAGTTTCCC

	AATCTTCCTTATTATATTGATGGTGATGTTAAATTAACAC AGTCTATGGCCATCATACGTTATATAGCTGACAAGCACAA CATGTTGGGTGGTTGTCCAAAAGAGCGTGCAGAGATTTCA ATGCTTGAAGGAGCGGTTTTGGATATTAGATACGGTGTTT CGAGAATTGCATATAGTAAAGACTTTGAAACTCTCAAAGT TGATTTTCTTAGCAAGCTACCTGAAATGCTGAAAATGTTC GAAGATCGTTTATGTCATAAAACATATTTAAATGGTGATC ATGTAACCCATCCTGACTTCATGTTGTATGACGCTCTTGAT GTTGTTTTATACATGGACCCAATGTGCCTGGATGCGTTCC CAAAATTAGTTTGTTTTAAAAAACGTATTGAAGCTATCCC ACAAATTGATAAGTACTTGAAATCCAGCAAGTATATAGC ATGGCCTTTGCAGGGCTGGCAAGCCACGTTTGGTGGTGGC GACCATCCTCCAAAA

APPENDIX B

Primers used in this study

PRIMER NAME	*DNA SEQUENCE (5'-3')*
JO1	ACCGTTTTTATTGATGGTTGTGCGCTTAAG GCTGCTCACGGTCACCTG
JO2	CACCACCACCACCACGGTGGCGGTGGATCC CAGGTGCAGCTGCAGGAAAG
JO5	GGTGGTGGCGACCATCCTCCAAAAGGATCC ATGACTGAAATCGTTGCAGATAAAAC
JO6	TCTCAGTGGTGGTGGTGGTGGTGCTCGAGTC ATCAGACTTCAGGTACCTCAAAGAG
PREA24	TCTGTTCCAGGGGCCCCTGGGATCCGGTGG CGGTGGTAGCGAAAACCTGTACTTTCAGGGCGG TG
MKL2	CCGTTTTTATTGATGGTTGTGCGCTT AAGATTCATCAGCTGGGTGGCTT
pZA Ag43 atc FWD	CTTAAGCGCACAACCATCAATAAAAACGGTCG
pZA Ag43 atc REV	CACGGTGGCGGTGGATCC
JO11	CGCTGCTGCTGGTCTGCTGCTCCTCGCT GCCCAGCCGGCGATGGCCGGTGGCGGTGGATCCATG

JO12	TTCGTTTTATTTGATGCCACGCGTCTCGAGTCA TTAGTGGTGGTGGTGGTGGT
PREA29	ACGCGTGGCATCAAATAAAACGAAA
PREA78	CTTTTTTTCATGGTACCCTCCTTCAGA TCTTTTGAATTCTTTTCTCTATC
JO29	AAGAATTCAAAAGATCTGAAGGAGGGTACCATGAA AAAAAGAGGGGCGTT

APPENDIX C

SEQUENCING DATA

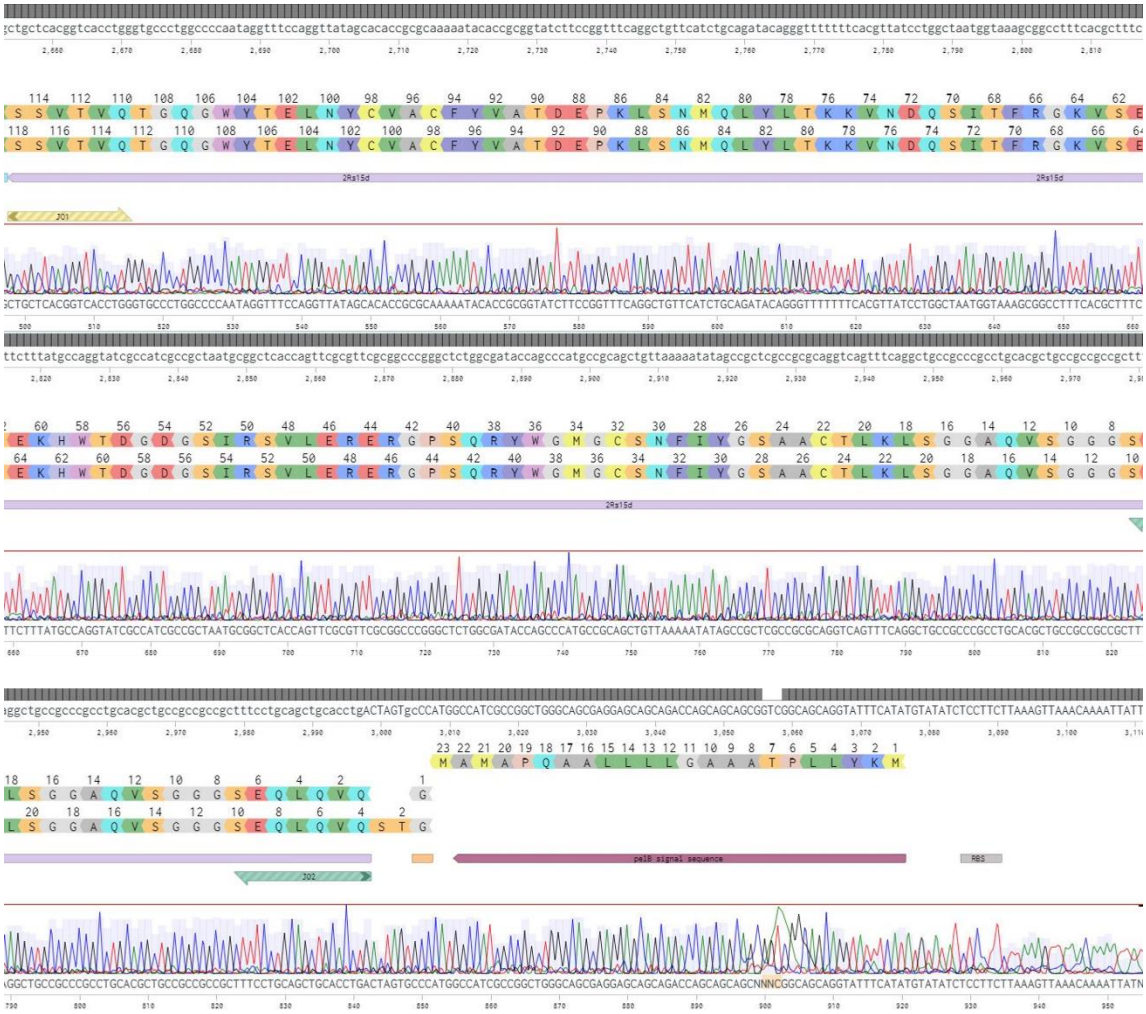

Figure 46. Alignment of pET22b T7-LacO pelB 2Rs15d Ag43 AmpR with sanger sequencing result via Benchling.

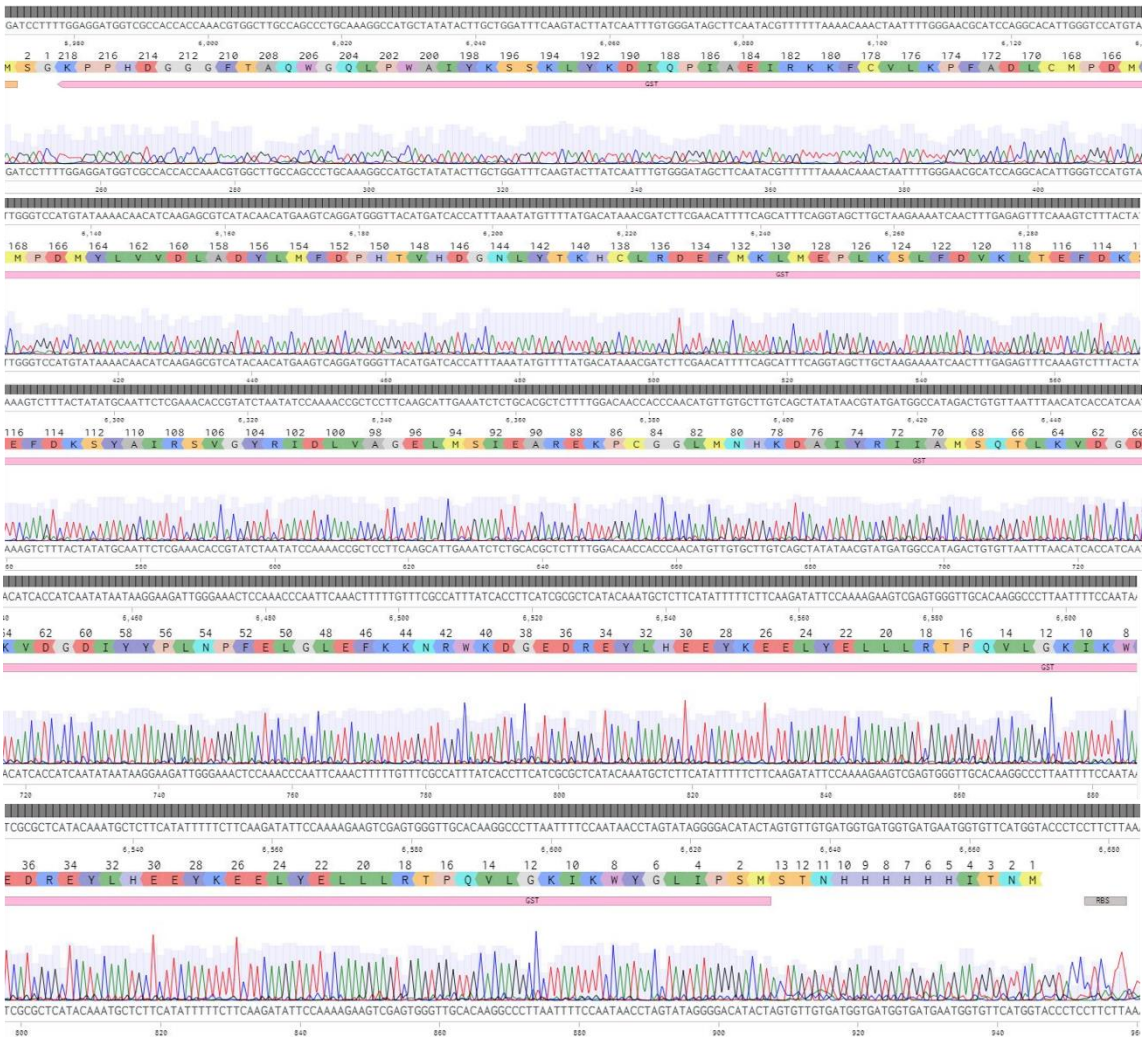

Figure 47. Alignment of pET22b T7-LacO GST HlyE 6xHis AmpR to sanger sequencing result (GST verification) via Benchling.

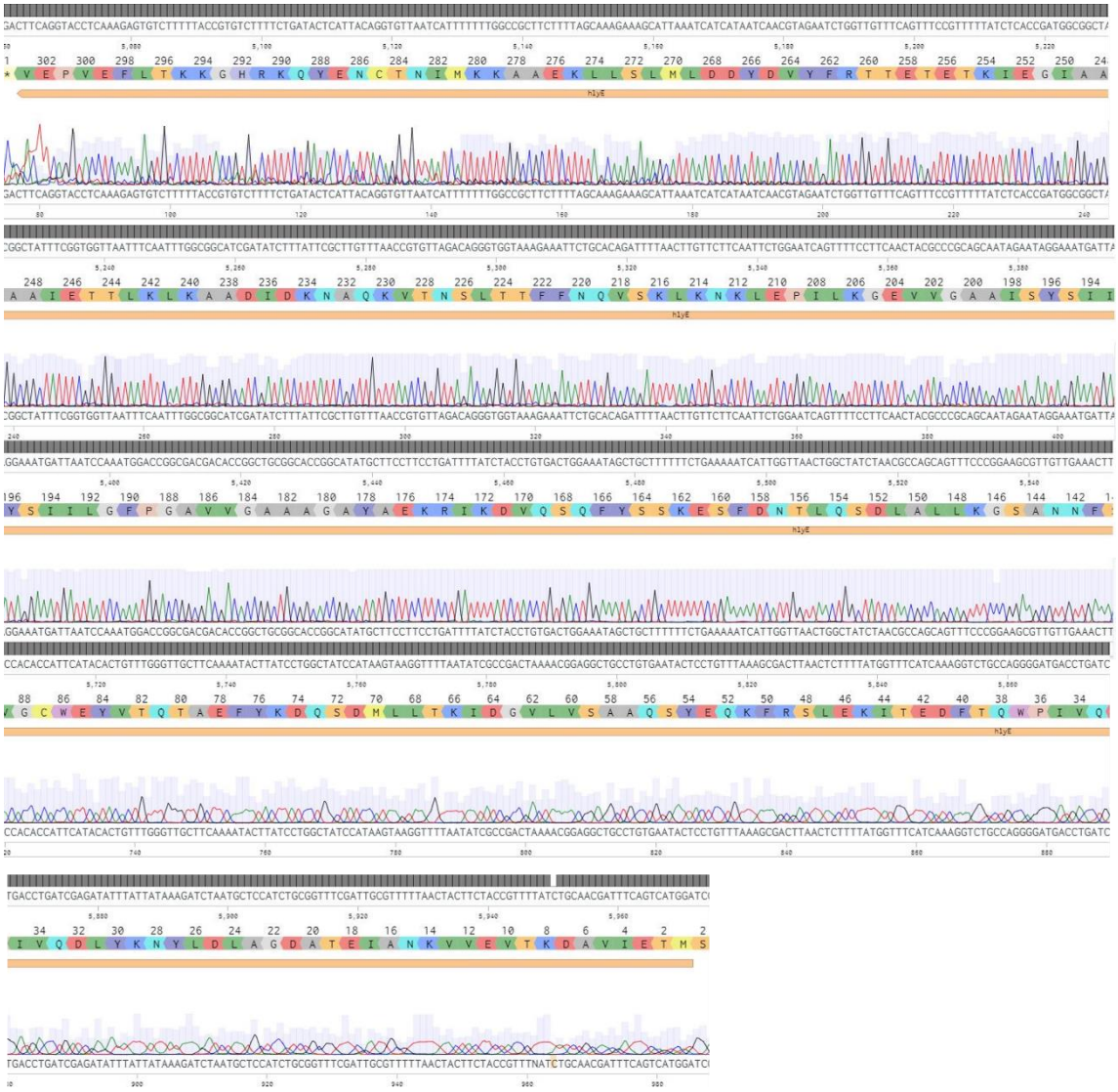

Figure 48. Alignment of pET22b T7-LacO GST HlyE 6xHis AmpR to sanger sequencing result (HlyE verification) via Benchling.

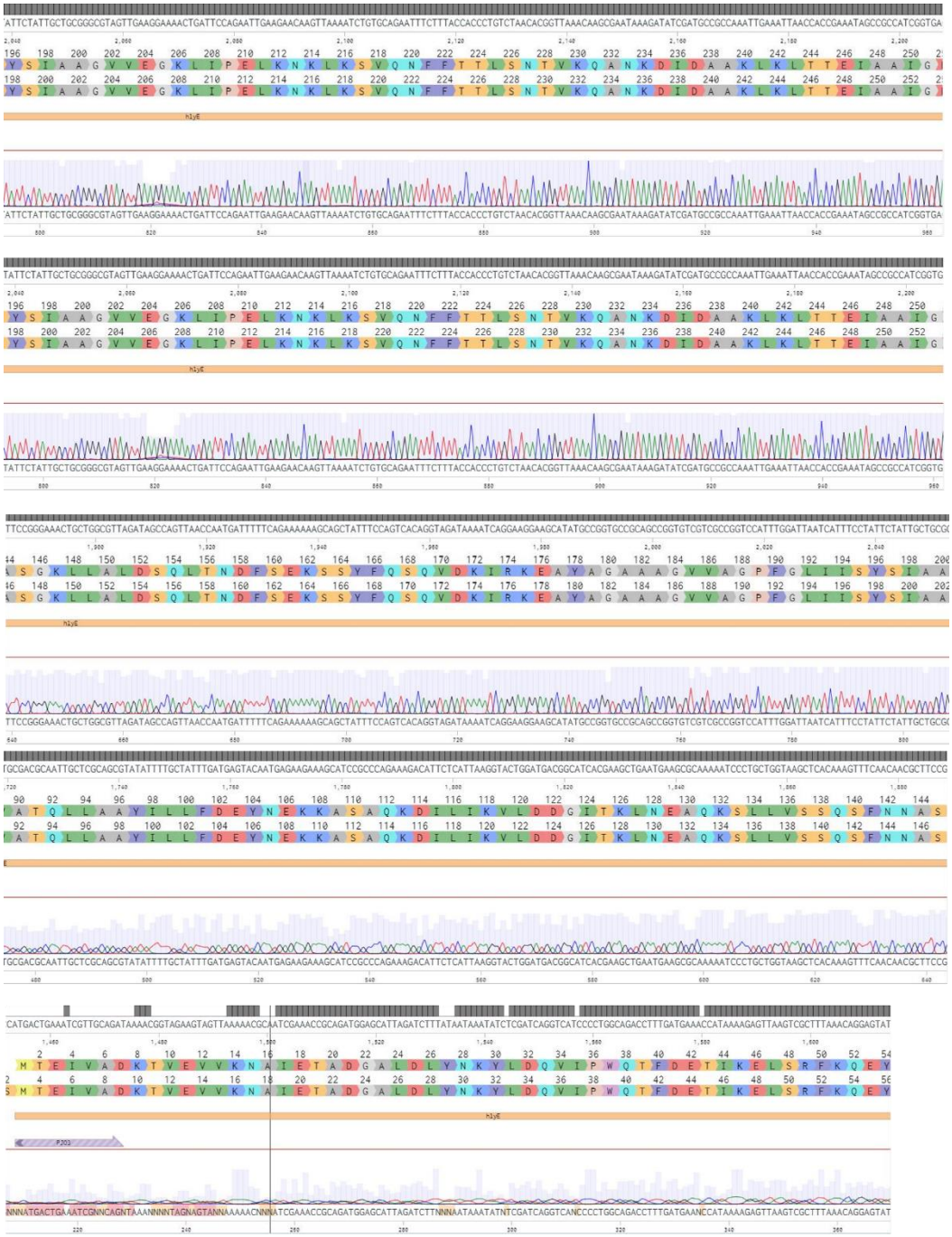

Figure 49. Alignment of pZA pL-TetO YebF HlyE 6xHis AmpR to the sanger sequencing result via Benchling.

Figure 50. Alignment of pET22b T7-LacO pelB 6xHis 2Rs15d Ag43 AmpR sequencing result using Geneious program.

Figure 51. Alignment of pZA native pTetO HlyE Yebf 6xHis CmR sequencing result using Geneious program.

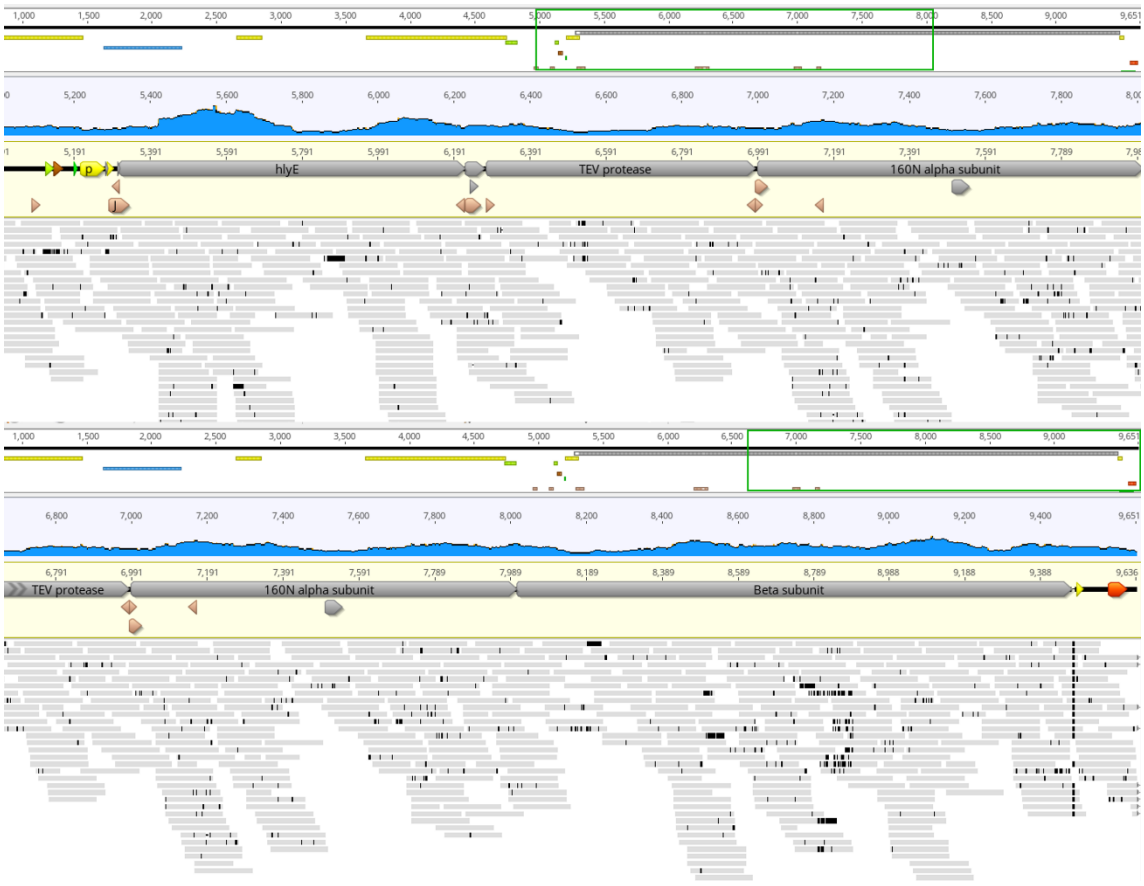

Figure 52. Alignment of pET22b 6xHis HlyE TEV-Linker TEV Protease Ag43 AmpR sequencing result using Geneious program.

APPENDIX D

Plasmid Maps

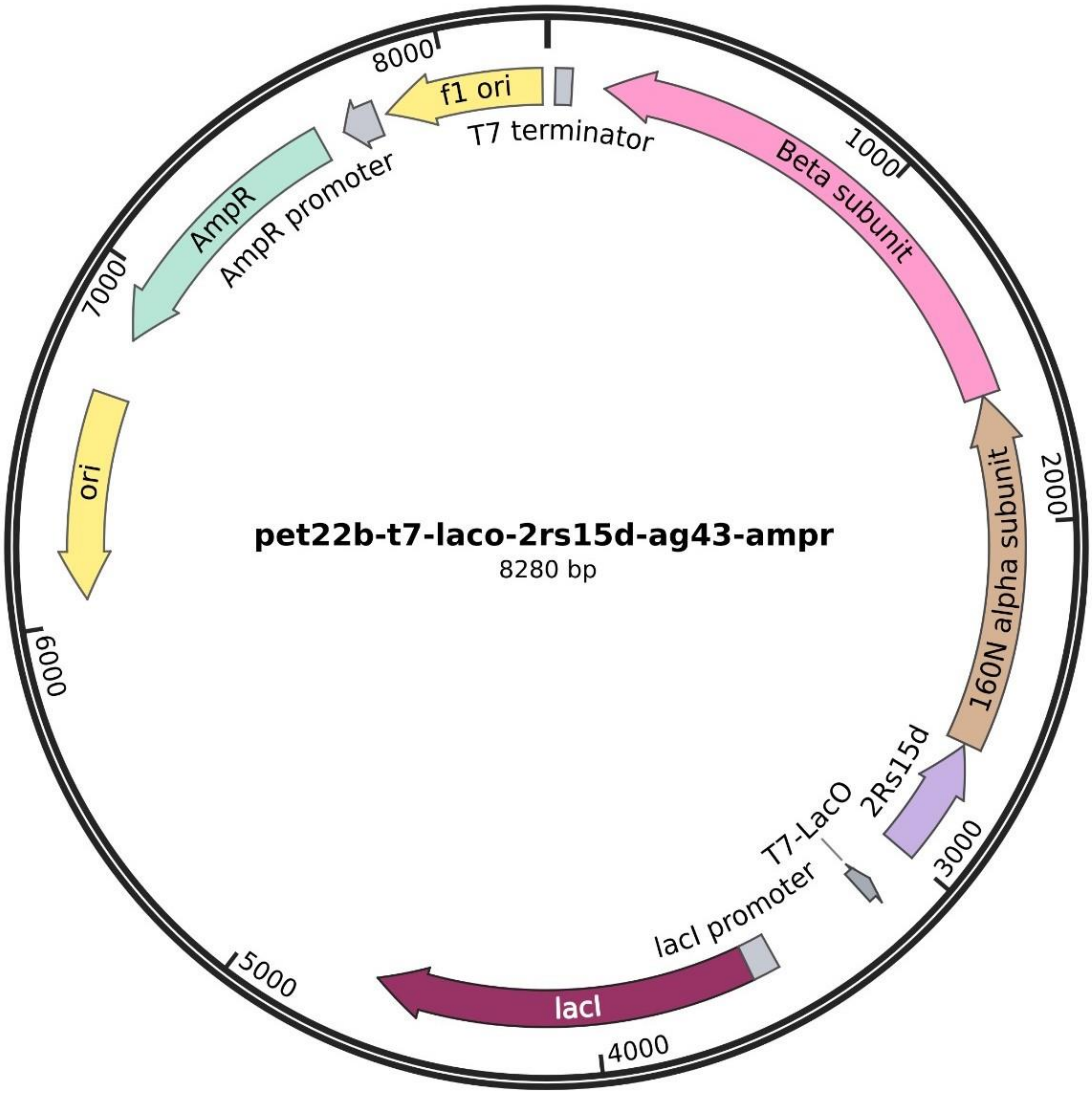

Figure 53. Plasmid map of pET22b T7 lacO 2Rs15d Ag43 AmpR vector.

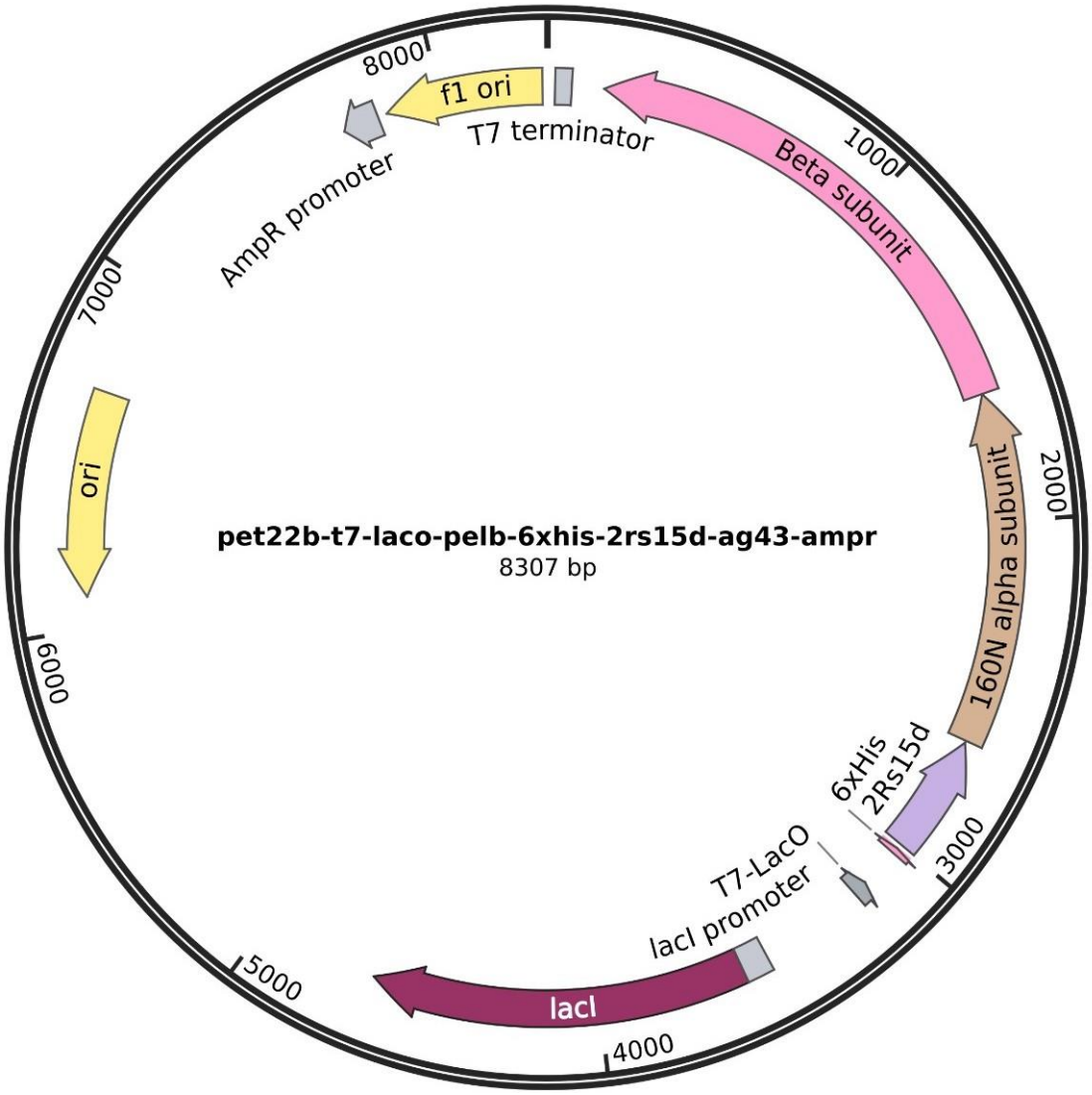

Figure 54. Plasmid map of pET22b T7 lacO 6xhis 2Rs15d Ag43 AmpR vector.

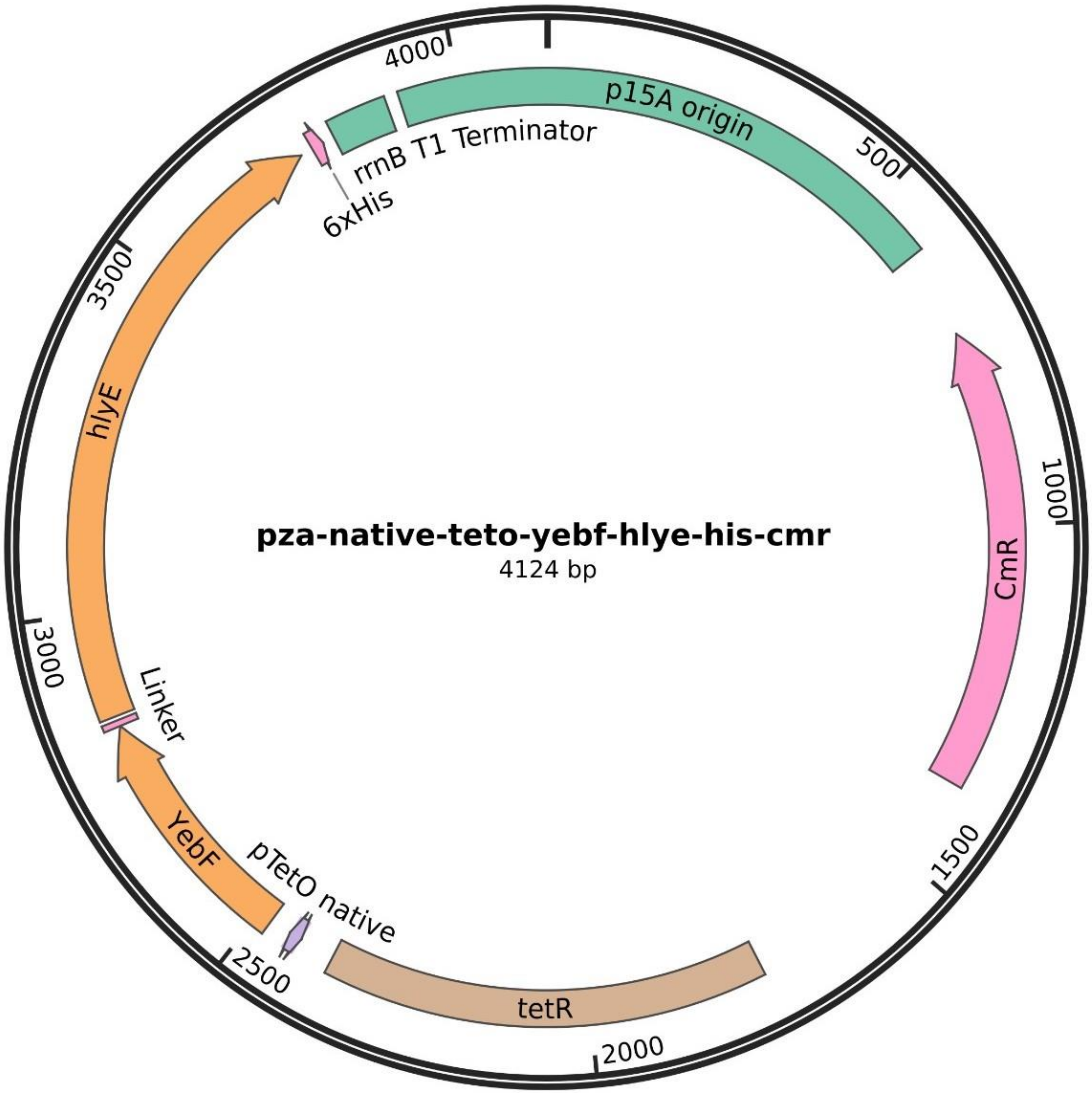

Figure 55. Plasmid map of pZA native tetO YebF HlyE 6xhis CmR vector.

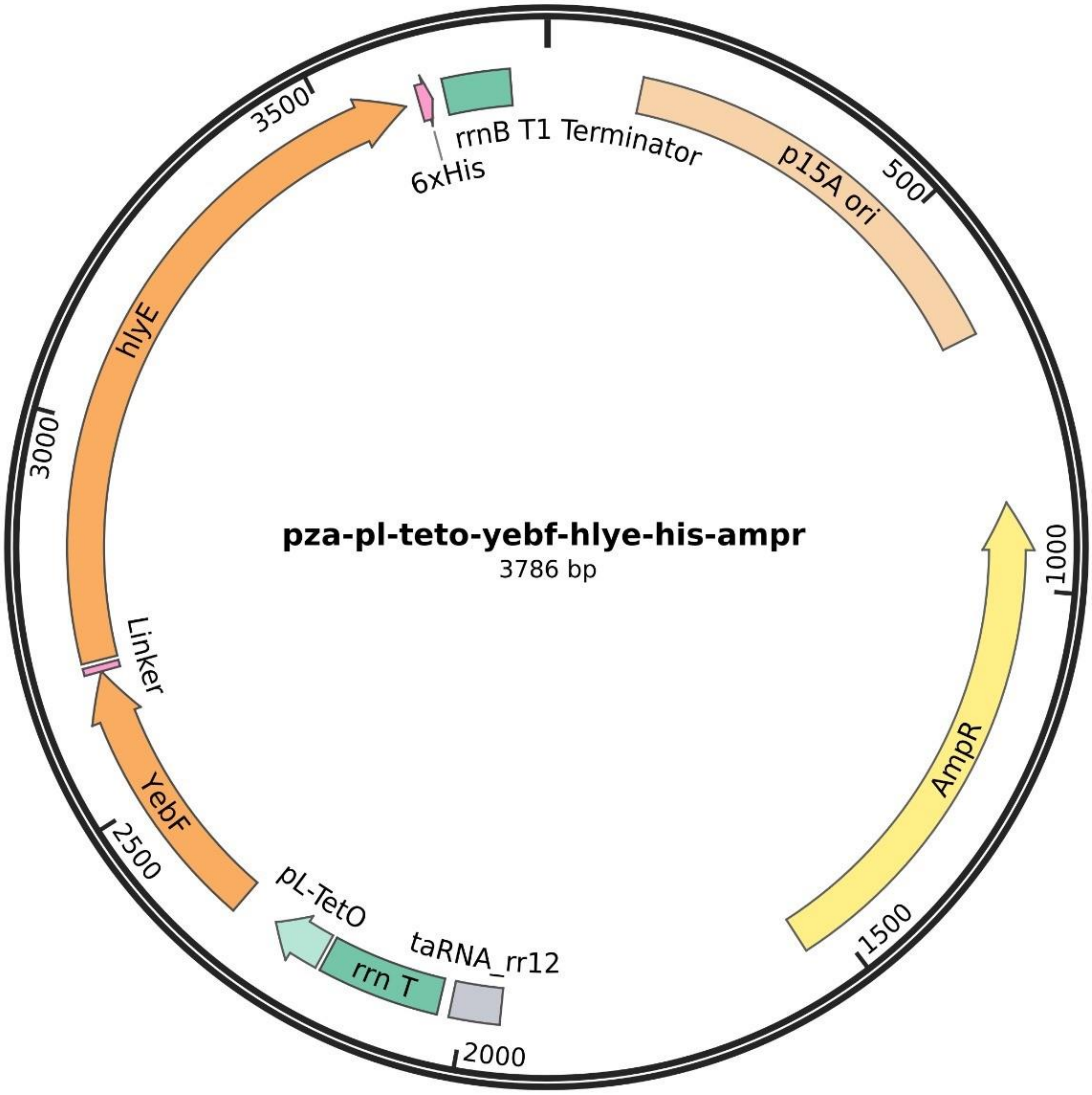

Figure 56. Plasmid map of pZA pL-tetO YebF HlyE 6xhis AmpR vector.

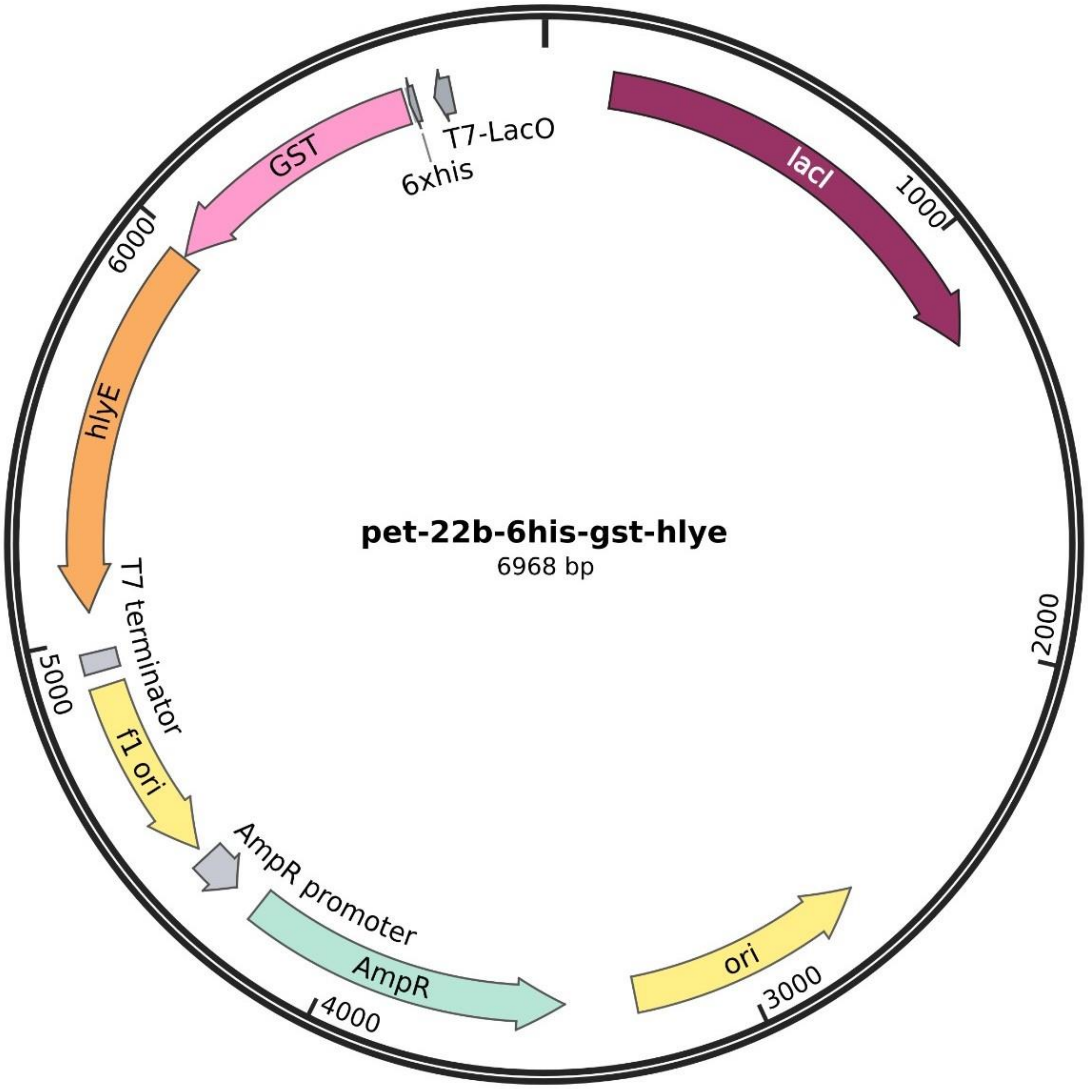

Figure 57. Plasmid map of pET22b T7 lacO GST 2Rs15d 6xhis AmpR vector.

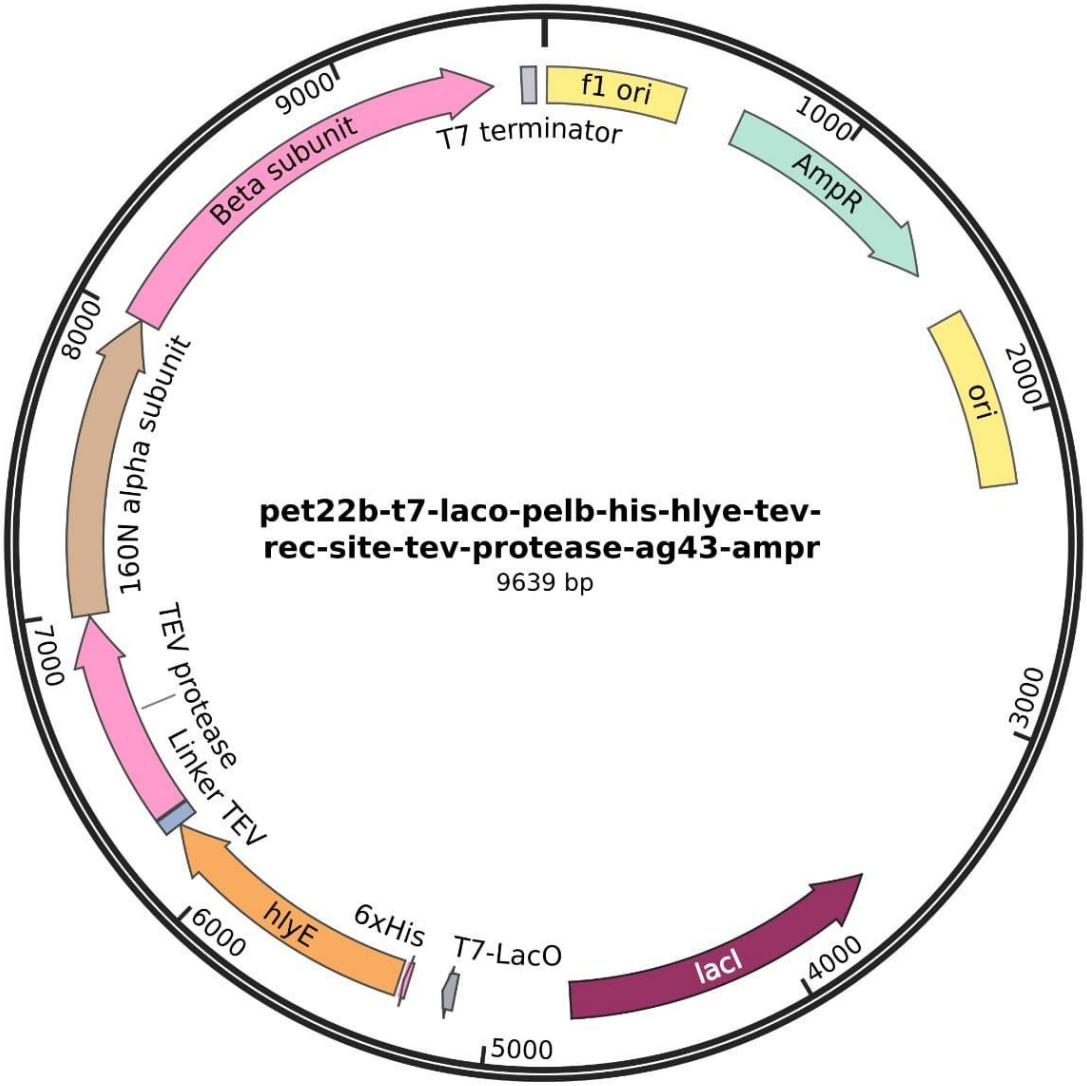

Figure 58. Plasmid map of pET22b T7 lacO 6xhis HlyE TEV rec site TEV Protease Ag43 AmpR.

APPENDIX E

Additional recipes and reaction conditions

Table 3. 1,3X Gibson Reaction Mix.

Component	Quantity
Nuclease free water	216,75 µL
5X Isothermal buffer	100 µL
Taq ligase	50 µL
Phusion polymerase	6,25 µL
T5 exonuclease	2 µL

Table 4. Gibson Assembly Reaction.

Component	Quantity
Gibson Reaction Mix	7,5 µL
Backbone DNA	50 ng
Insert DNA	Equimolar to backbone DNA
Double distilled water	Variable (total volume is 10 µL)

Table 5. Liquid Broth Medium (LB) Recipe (for 1 L).

Component	Quantity
Yeast extract	5 g
Tryptone	10 g
NaCl	10 g
Agar	15 g
Double distilled water	1000 mL

Table 6. Cultivation Media for Jimt1 and MDA MB 231 mammalian cells.

Component	Concentration
FBS (Fetal Bovine Serum)	10 % (v/v)
Antibiotic (Pen/Strep)	1 % (v/v)
L-Glutamine	1 % (v/v)
Low Glucose DMEM	88 % (v/v)